ИССЛЕДОВАНИЯ КОНДЕНСИРОВАННЫХ СРЕД НА РЕАКТОРЕ ИБР-2:
ИЗ ПРОШЛОГО В БУДУЩЕЕ

Д.П. Козленко

Лаборатория нейтронной физики им. И.М.Франка,
Объединенный институт ядерных исследований, 141980 Дубна

IBR-2 High Flux Pulsed Reactor (FLNP JINR)

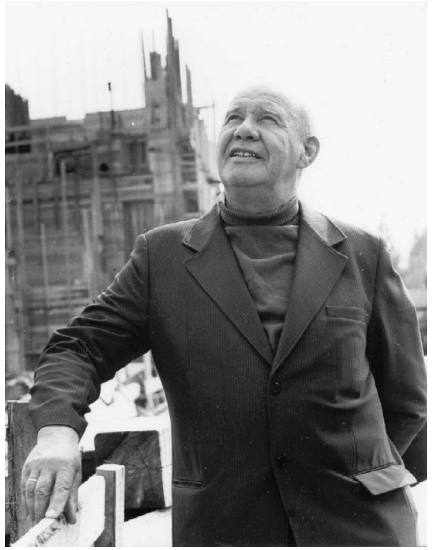

D.I.Blokhintsev

Put into operation since 1984

Based on experience with older generations IBR-1 (1960), IBR-30 (1969)

Thermal neutron flux:	$5 \cdot 10^{15}$ n/cm^2/s
Repetition rate:	5 Hz
Thermal neutron pulse width	340 μs

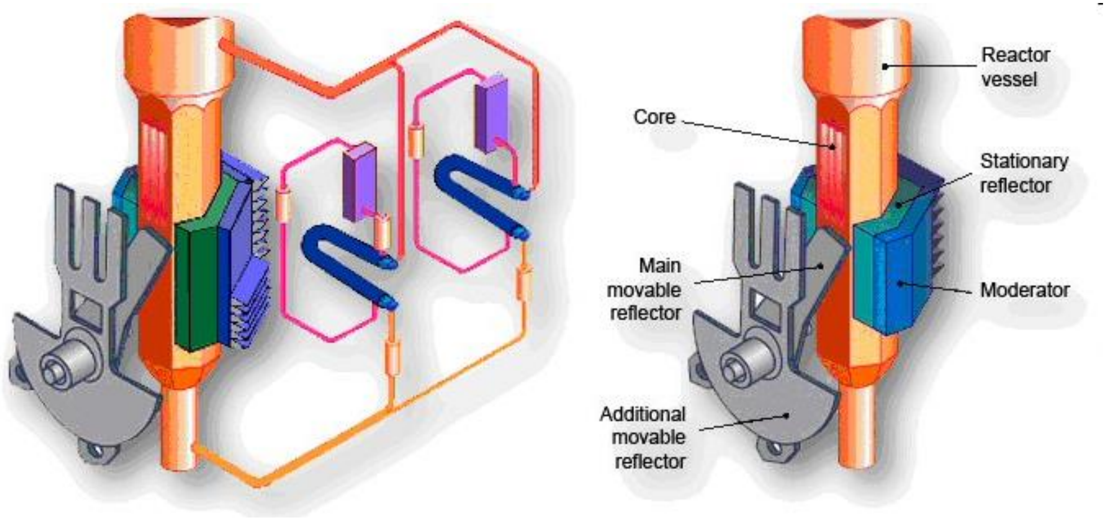

In 1980th IBR-2 was the pulsed neutron source with the largest thermal neutron flux for scientific research in the world

KENS (KEK, Japan):	$1 \cdot 10^{14}$ n/cm^2/s, 15 Hz, 30 μs (1980)
IPNS (ANL, USA):	$3 \cdot 10^{14}$ n/cm^2/s, 30 Hz, 30 μs (1981)
MLNSC (LANL, USA):	$7 \cdot 10^{14}$ n/cm^2/s, 20 Hz, 30 μs (1985)
ISIS (RAL, UK):	$1 \cdot 10^{15}$ n/cm^2/s, 50 Hz, 30 μs (1985)

Research Programme in Condensed Matter Physics using Neutron Scattering

Initiated in late 1960th

I.M. Frank (1908 - 1990)

F.L. Shapiro (1915 - 1973)

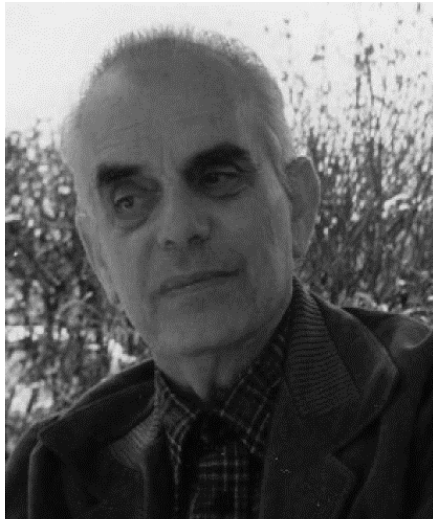

B.Buras (1915 - 1994)

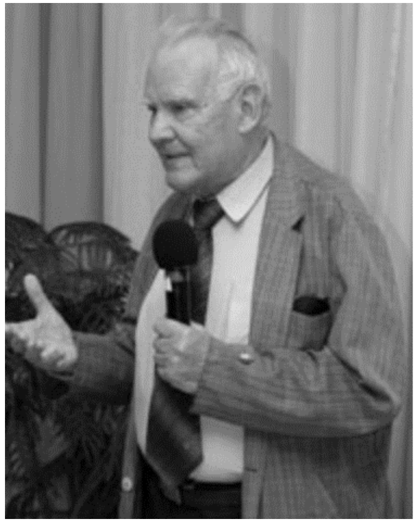

J.Janik (1927 – 2012)

In FLNP, Condensed Matter Physics Department was established in 1972

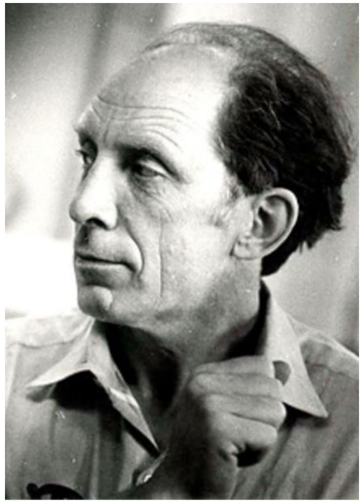

Yu.M. Ostanevich (1936 – 1992)

IBR-2 Spectrometers for Condensed Matter Research in the Beginning (1984)

- DN-2 diffractometer (A.M.Balagurov, A.I.Beskrovny, B.N.Savenko, V.I.Gordeliy)
- MURN Small angle neutron scattering spectrometer (Yu.M.Ostanevich, L.Cser, A.B.Kunchenko)
- NSHR Texture diffractometer (K.Feldmann, K.Walter)
- KDSOG-M inelastic neutron scattering spectrometer in inverted geometry (G.Baluka, I.Natkaniec, A.V.Belushkin)
- DIN-2PI Inelastic neutron scattering spectrometer in direct geometry (IPPE, V.A.Parfenov, V.G.Liforov, A.G. Novikov, A.V.Puchkov, E.L.Yadrovsky et al.)
- SPN-1 Polarized neutron spectrometer (D.A.Korneev)
- KORA Spectrometer for correlation analysis (N.Kroo, P.Pacher)
- DIFRAN Diffractometer with perfect crystals (Yu.A.Aleksandrov)

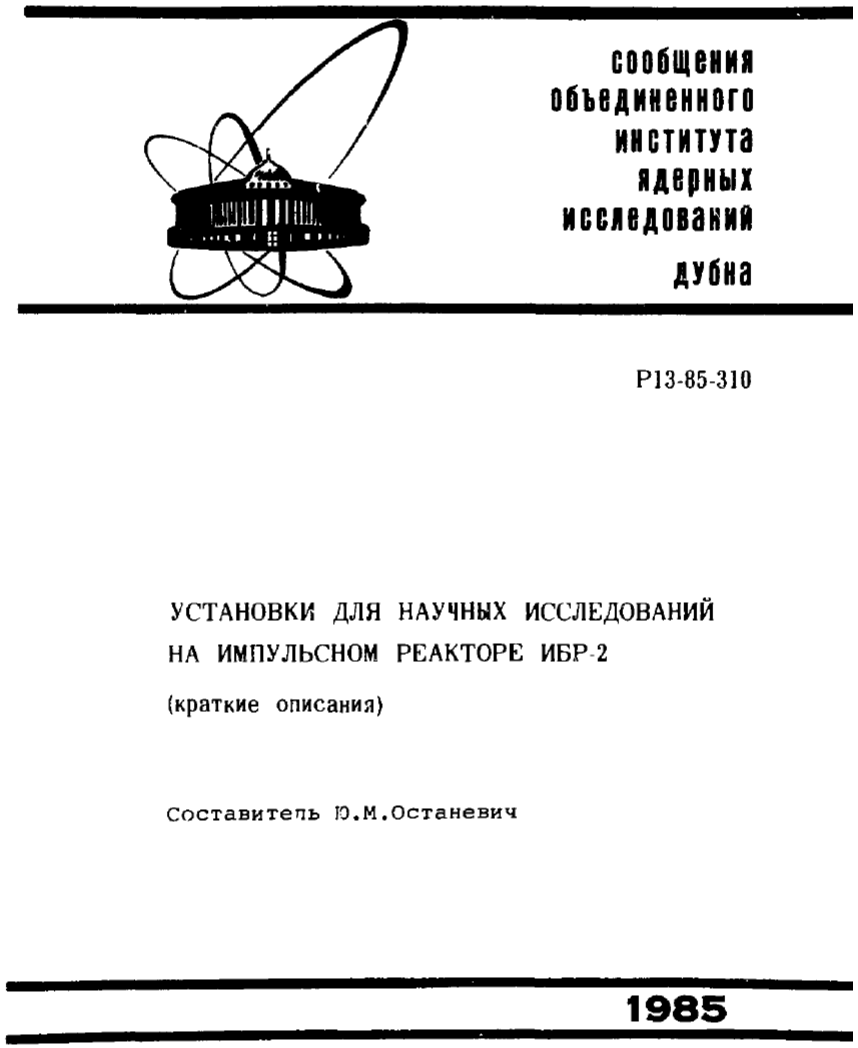
сообщения
объединенного
института
ядерных
исследований
дубна

Р13-85-310

УСТАНОВКИ ДЛЯ НАУЧНЫХ ИССЛЕДОВАНИЙ
НА ИМПУЛЬСНОМ РЕАКТОРЕ ИБР-2
(краткие описания)

Составитель Ю.М.Останевич

1985

Advantages of time-of flight neutron scattering

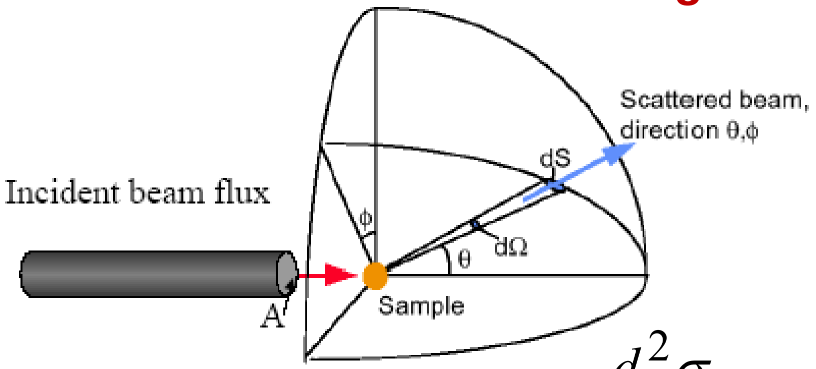

Scattering law:

$$\frac{d^2\sigma}{d\Omega d\omega} = \frac{k}{k_0}\frac{1}{2\pi}\iint d\vec{r}dt\, e^{i(\vec{Q}\vec{r}-\omega t)}G(\vec{r},t) = \frac{k}{k_0}S(Q,\omega)$$

$Q(\lambda, \theta), \omega(\lambda)$

Real time neutron diffraction (DN-2, since 1985)

Minimal measurement times from 0.2 s, typical values *t* ~ 0.5 – 5 min.
In other world neutron centers even nowdays, typical values *t* ~ 1-5 min.

G.M.Mironova (1944-2022)

Time evolution of structural phases in ice during the heating of the phase VIII from 94 to 290 K with a rate of 5K/min

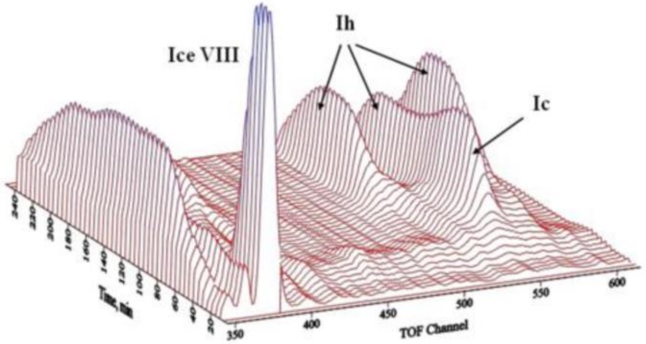

A.M.Balagurov, O.I.Barkalov et al, JETP Lett. 53, 30 (1991).

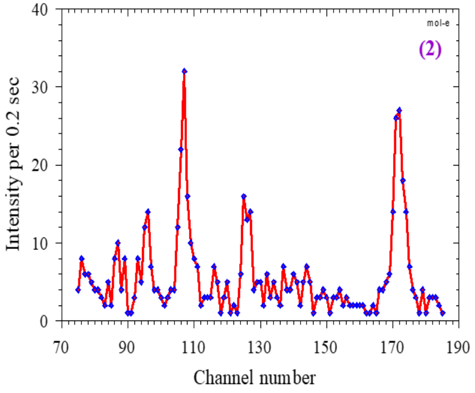

Diffraction pattern of NI measured during 1 neutron pulse (0.2 s).

Development of polarized neutron scattering methods, including reflectometry (SPN-1, since 1985)

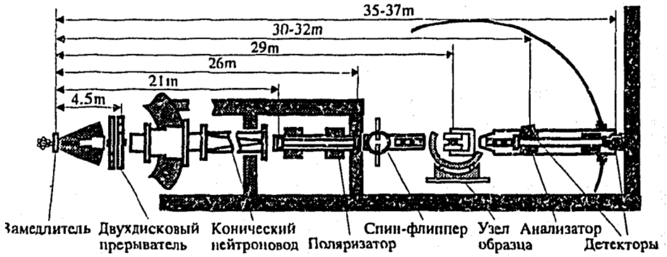

D.A.Korneev (1946-2002)

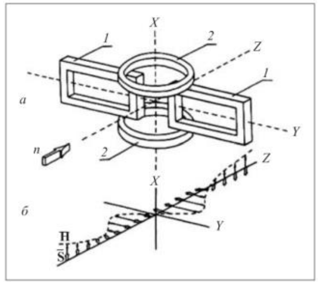

Korneev spin-flipper. D.A.Korneev. NIM 169, 65 (1980).

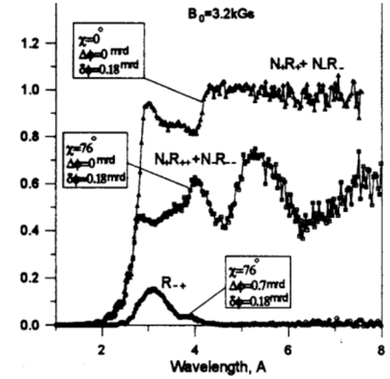

Wavelength dependence of reflection coefficients for FeCo anisotropic thin film in specular and off-specular direction.

Neutron diffraction in pulsed magnetic fields (SNIM-2, since 1988)

V.V.Nietz (1937-2020)

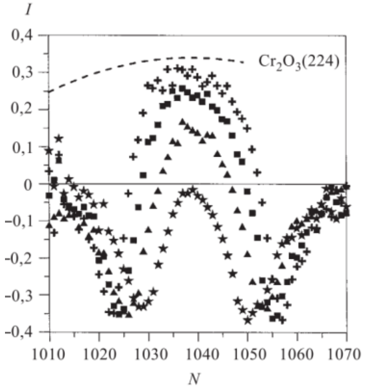

Magnetic field pulse amplitude: up to 12 T
Magnetic field pulse duration: 0.5 – 3 ms

Spin flop transitions of Cr_2O_3 in pulsed magnetic fields

Relative intensity $(I_H-I_0)/I_0$ for 224 peak, derived from neutron diffraction patterns of Cr_2O_3 in pulsed magnetic fields up to 7.1 T. D.Georgiev, V.V.Nietz et al., JINR Communication P14-92-400 (1992).

First experiments by neutron radiography, neutron activation analysis, development of mirror neutron guides (since 1985)

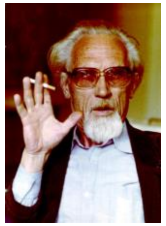

V.M.Nazarov (1931-1994)

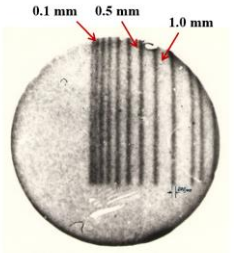

Cd plate with slits for resolution test

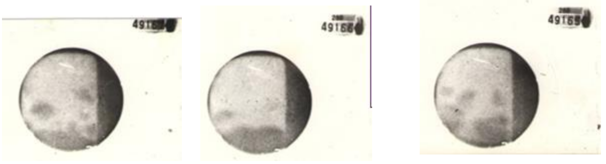

Time resolved experiment with boiling water

From Pioneering Results towards Establishing of Novel Research Directions

Diffraction studies of biological membranes

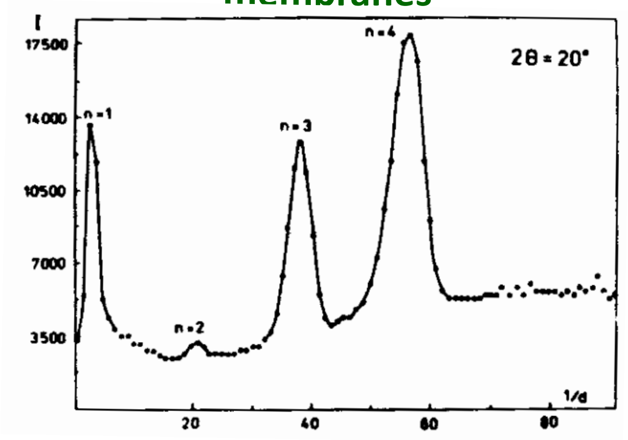

Diffraction pattern of DPL (DN-2)
A.M.Balagurov, V.I.Gordeliy, Краткие сообщения ОИЯИ 1- 84 (1984)

Domain structure of ferroelectrics and ferroelastics in external electric fields

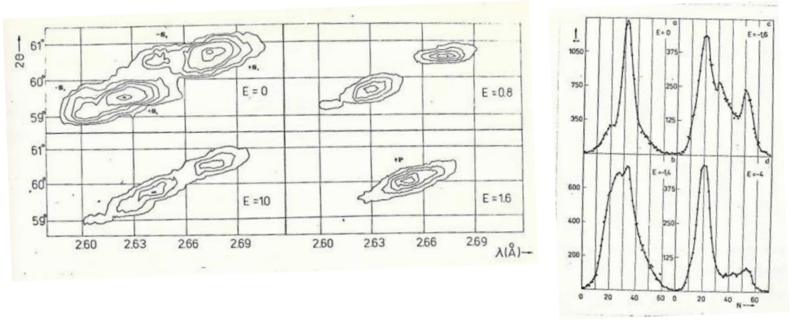

Intensity distribution around the (080) reflection of the KD_2PO_4 single crystal in applied electric fields and *T* = 210 K (DN-2). A.M.Balagurov, I.D.Dutt, B.N.Savenko, L.A.Shuvalov, Ferroelectrics 48, 163 (1983).

SANS studies of polyelectrolites

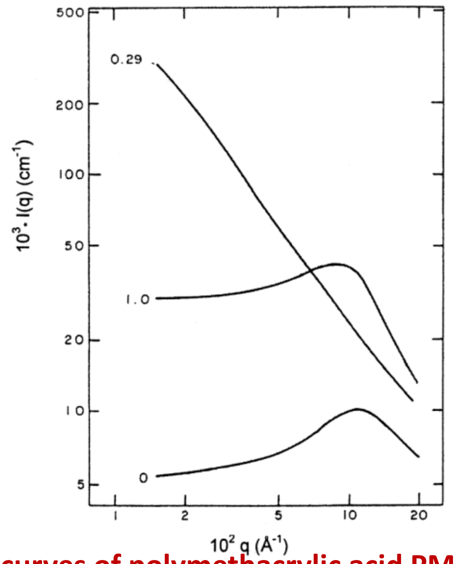

SANS curves of polymethacrylic acid PMA(H), PMA(D) and their mixture (MURN). J.Plestil, Yu.M.Ostanevich et al., Polymer 27, 39 (1986).

Vibrational dynamics of superionic conductors

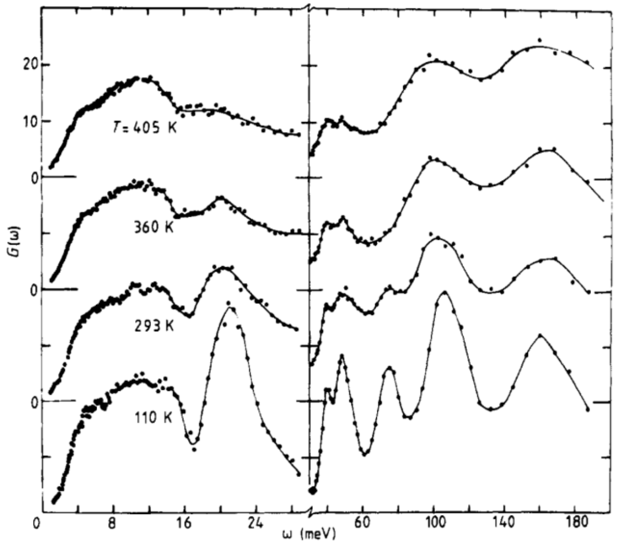

Spectral density of vibrational states of $CsHSeO_4$. A.V.Belushkin, I.Natkaniec, N.M.Plakida et al., J. Phys. C 20, 671 (1987).

Studies of Bose condensation of liquid He

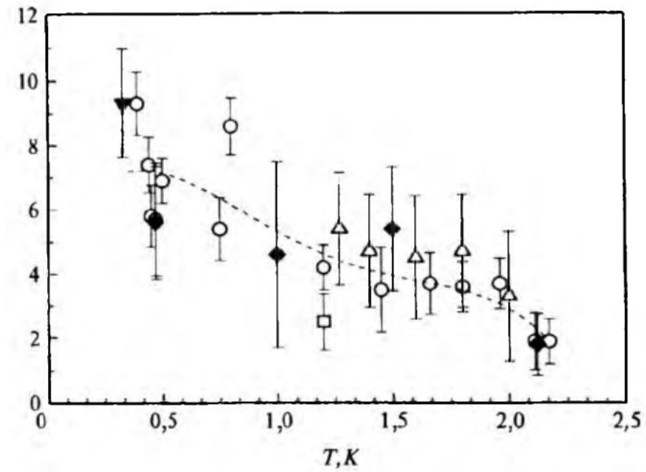

Experimental density of Bose condensate in liquid ^{4}He (DIN-2PI). I.V.Bogoyavlenskii, L.V.Karnatsevich, J.A.Kozlov, A.V.Puchkov, Physica B 176, 151 (1992).

Determination of magnetic field penetration depth into superconducting $YBa_2Cu_3O_7$ thin film

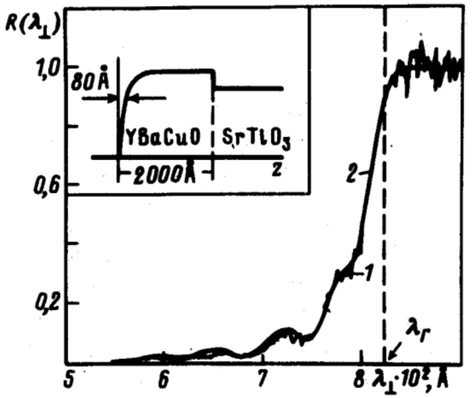

Reflection coefficient as a function of neutron wavelength component $\lambda_{\perp}$. S.V.Gaponov, E.B.Dokukin, D.A.Korneev et al., JETP Lett. 49, 277 (1989).

Development of High Resolution Fourier Diffractometry (1992-1994)

Collaboration FLNP JINR – PNPI – VTT (Finland) – IzfP (Germany)

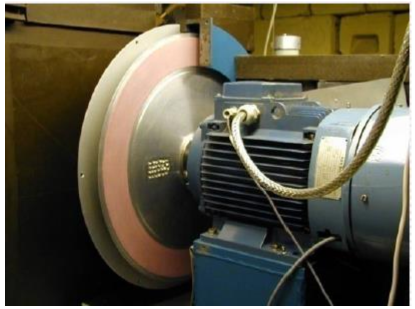

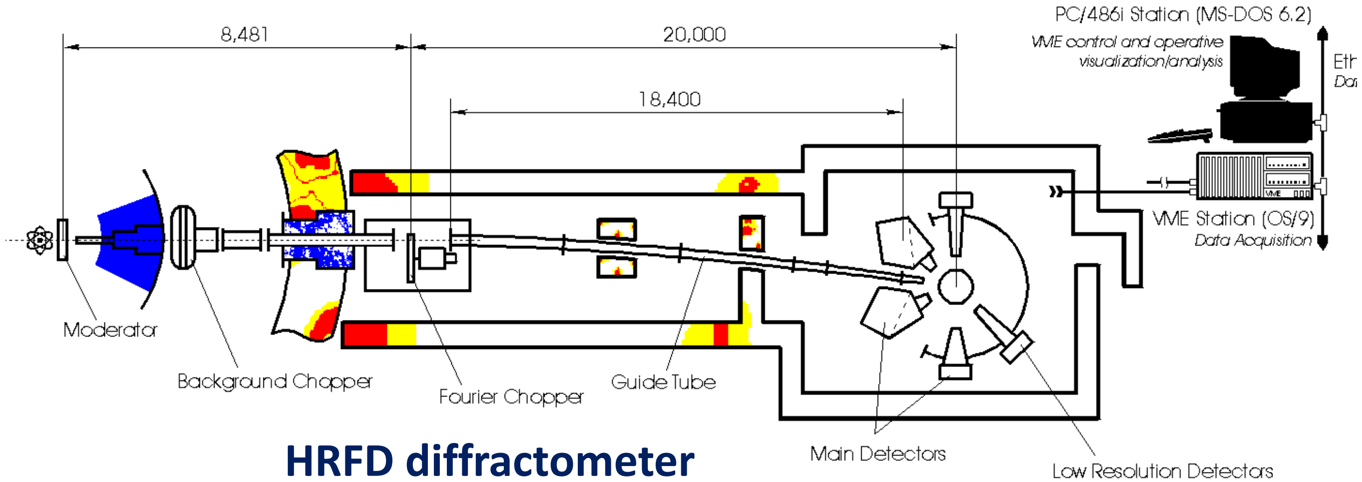

HRFD diffractometer

V.L.Aksenov, A.M.Balagurov, V.A.Trounov

P.Hiismaki

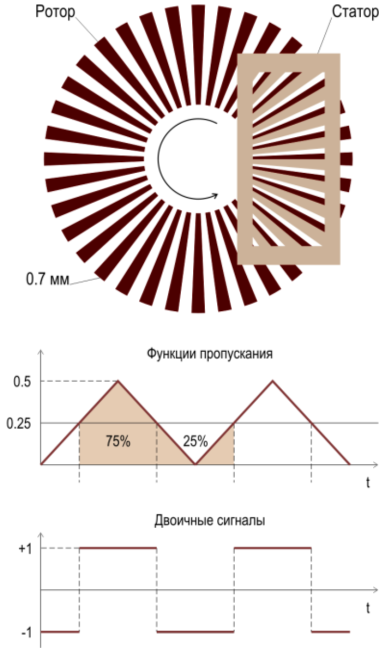

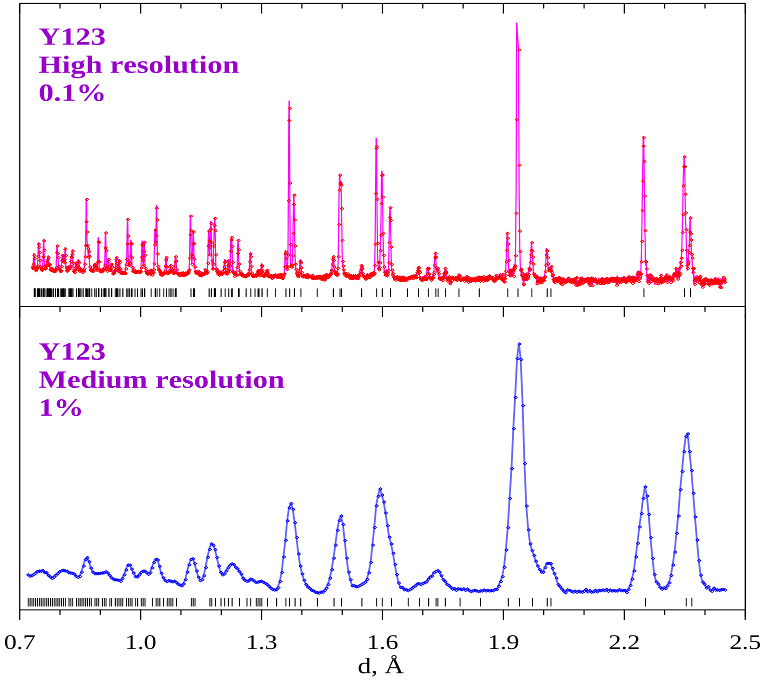

Neutron flux at sample position: 10^7 n/cm2/s

Resolution at d = 2 Å, 2θ =152⁰:
$\Delta d/d$ = 0.0008

D-spacing range in high resolution mode: 0.7- 4 Å

$\Delta t \approx 10$ μs

DN-12 Spectrometer for Studies of Microsamples

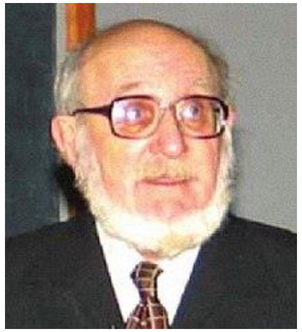

V.A.Somenkov
(1937 – 2018)

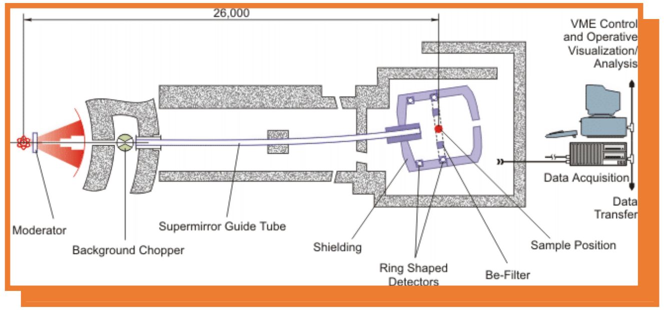

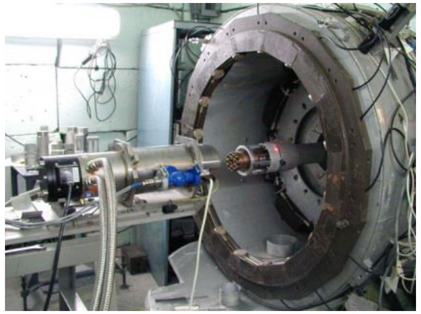

Starting configuration was created in 1993, final configuration in 1997, designed in collaboration with NRC Kurchatov Institute

V.L.Aksenov, A.M.Balagurov, B.N.Savenko, D.P.Kozlenko, V.A.Somenkov, V.P.Glazkov

- **Main: Diffraction mode**
- **Complementary: Inelastic incoherent scattering mode in inverted geometry**

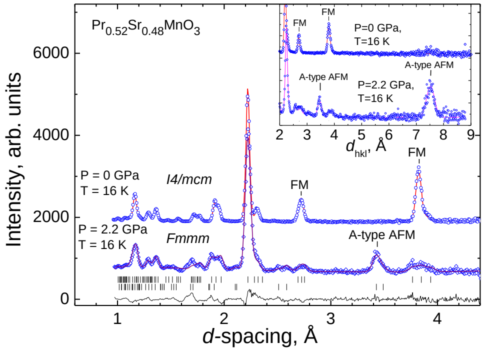

Neutron diffraction patterns of $Pr_{0.52}Sr_{0.48}MnO_3$ measured at selected pressures

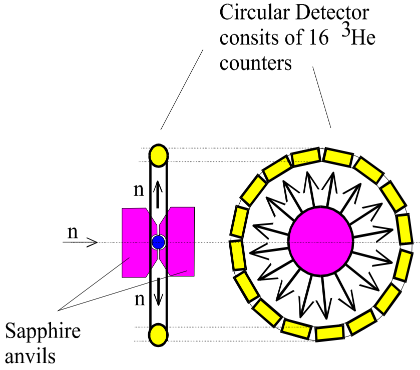

Sapphire anvil high pressure cell

Neutron flux at sample position: $2{\cdot}10^6$ n/cm^2/s

Diffraction mode

Resolution at d = 2 Å,

$2\theta = 90^0$: $\Delta d/d = 0.015$

$2\theta = 45^0$: $\Delta d/d = 0.022$

D-spacing range: 0.8 - 13 Å

Pressure range: 0 – 7 GPa

Temperature range: 10 – 300 K

Pressure induced hybridization of librational (L) and transverse optical (TO) modes frequencies in NH_4I at the orientational phase transition

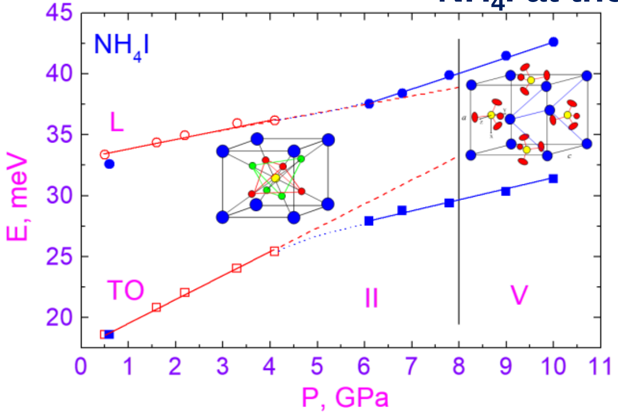

Pressure dependences of L and TO mode frequencies in NH_4I

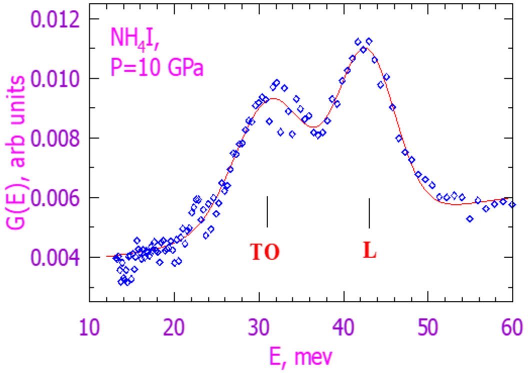

Generalized density of vibrational states of NH_4I at 10 GPa

V.P.Glazkov, D.P.Kozlenko et al., JETP Lett. 74, 415 (2001)

Further Development of IBR-2 Spectrometer Complex

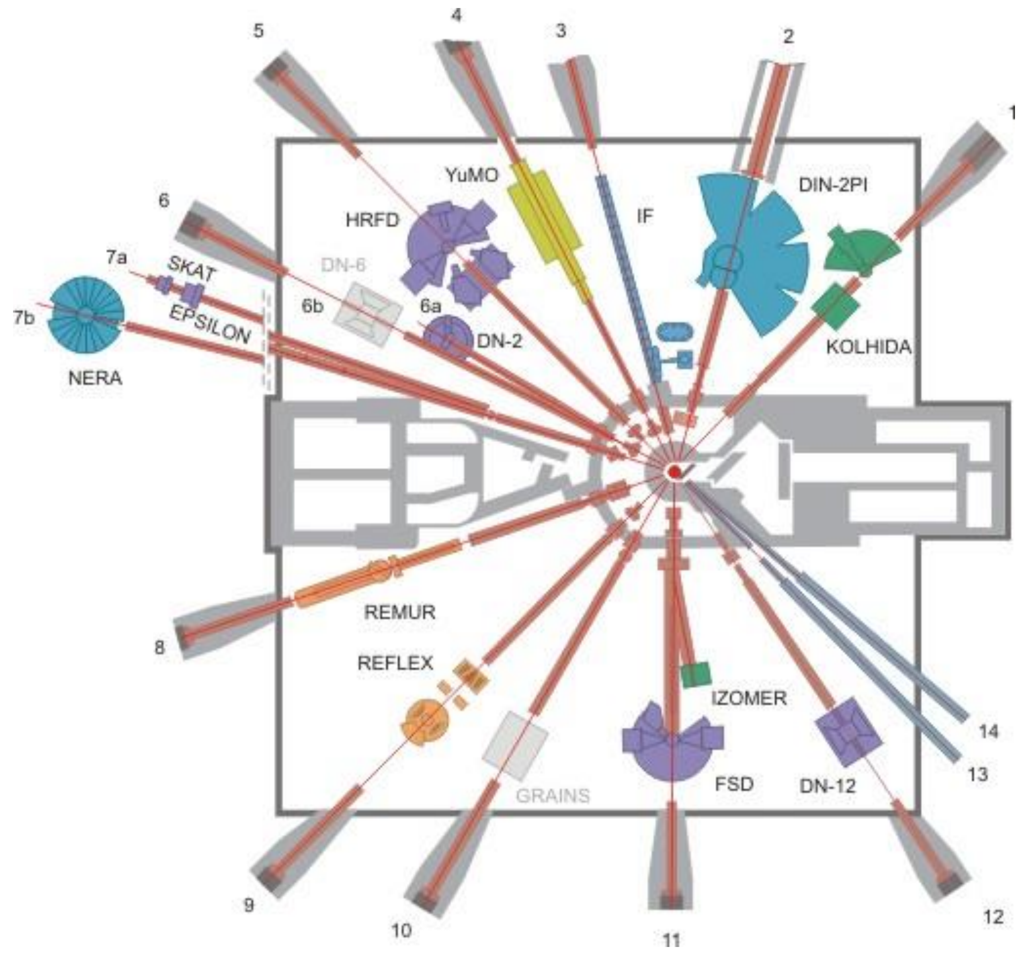

- **1992: Reflectometer with polarized neutrons REFLEX was created (D.A.Korneev, L.P.Chernenko, V.I.Bodnarchuk).**
- **1993: Inelastic neutron scattering spectrometer in inverted geometry NERA-PR was created (I.Natkaniec, S.I.Bragin, E.Brankowski, J.Mayer).**
- **1997: SKAT texture diffractometer was created (K.Ullemeyer, J.Heinitz, A.N.Nikitin, N.N.Isakov).**
- **1999-2005: Implementation of the two detector system at the small angle neutron scattering spectrometer, renamed as YuMO (A.I.Kuklin, A.Kh.Islamov, V.I.Gordeliy).**
- **2000: Fourier Stress Diffractometer FSD was created (G.D.Bokuchava, A.M.Balagurov, V.V.Zhuravlev).**
- **2000: Stress diffractometer for geophysical research EPSILON was created (K.Walter, C.Scheffzuek).**
- **2004: Reflectometer with polarized neutrons REMUR was created (Yu.V.Nikitenko, V.L.Aksenov, H.Lauter, V.V.Lauter-Pasyuk, A.V.Petrenko).**

2000: Государственная премия РФ за развитие и реализацию новых методов структурной нейтронографии по методу времени пролета на импульсных и стационарных реакторах

В.Л.Аксенов, А.М.Балагуров, В.В.Нитц, Ю.М.Останевич (ЛНФ ОИЯИ), В.А.Кудряшев, В.А.Трунов (ПИЯФ), В.П.Глазков, В.А.Соменков (НИЦ “Курчатовский институт”)

The Main Research Directions in 1990th – 2000th

- Neutron diffraction investigations of the structure and properties of new crystalline materials,
- Investigations of noncrystalline materials and liquids by small-angle neutron scattering,
- Neutron scattering studies of systems with complex surface,
- Investigations of atomic dynamics of condensed matter by inelastic neutron scattering,
- Investigations of texture and properties of rocks and minerals by neutron diffraction in a wide range of temperatures and pressures;
- Investigations of interrelation of textures and stresses in bulk materials

Structural Features of Hg-based Superconductors $HgBa_2Ca_{n-1}Cu_nO_{2n+2+\delta}$

V.L.Aksenov, A.M.Balagurov, V.V.Sikolenko et al., Phys. Rev. B 55, 3966 (1997), A.M.Abakumov, V.L.Aksenov et al. Phys. Rev. Lett. 80, 385 (1998), K.A.Lokshin et al., Phys. Rev. B 63, 064511 (2001), collaboration FLNP JINR – MSU

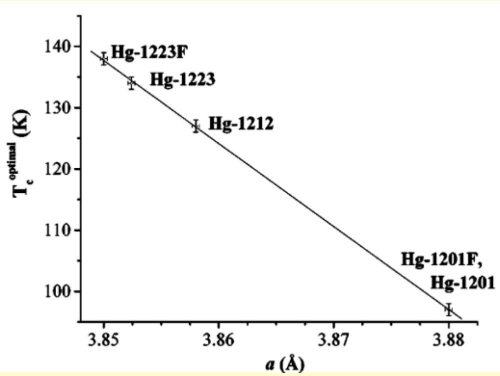

Dependence of optimal of T_c on *a* lattice parameter in fluorinated and non-fluorinated $HgBa_2Ca_{n-1}Cu_nO_{2n+2+\delta}$ (n = 1,2,3)

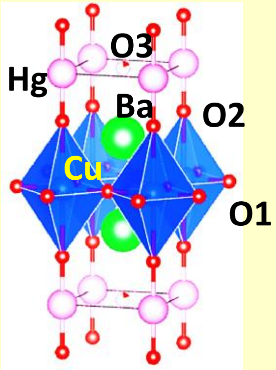

Crystal structure of $HgBa_2CuO_{4+\delta}$ (Hg-1201)

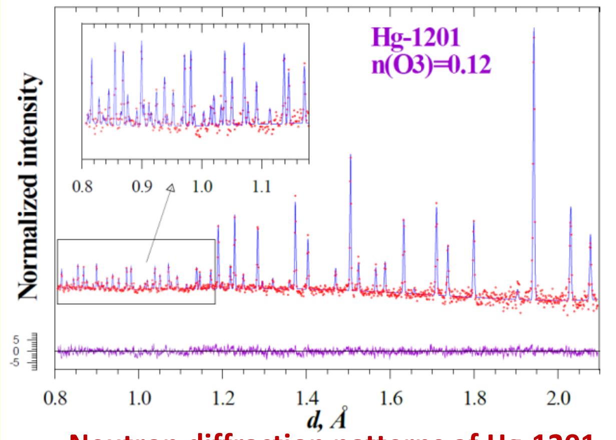

Neutron diffraction patterns of Hg-1201, measured with HRFD.

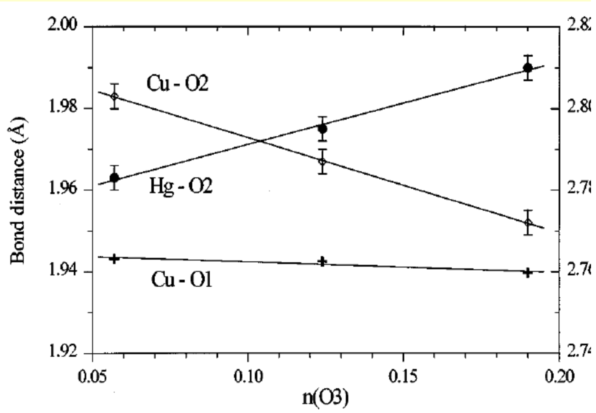

Bond distances as a function of extra oxygen content.

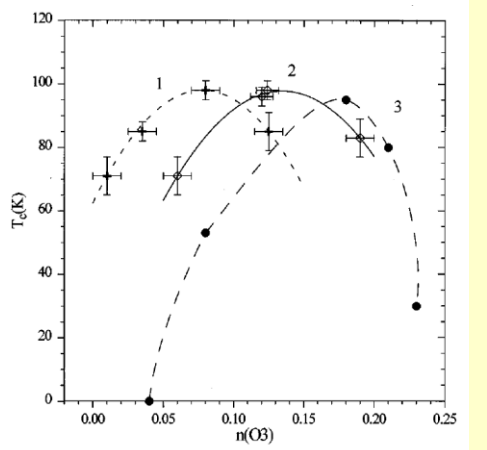

Behavior of T_c as a of extra oxygen content.

Frustrated Low-Dimensional Magnetism Under Extreme Conditions (High Pressure)

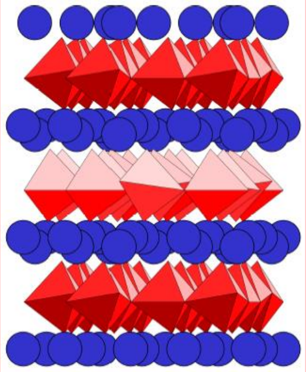

Crystal structure of multiferroic hexagonal $RMnO_3$

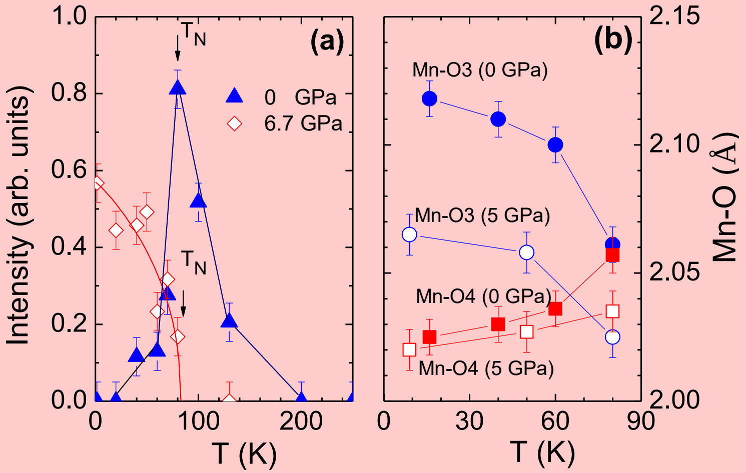

Temperature dependences of the magnetic diffuse scattering (left) and Mn-O bond lengths (right) in $YMnO_3$ at selected pressures

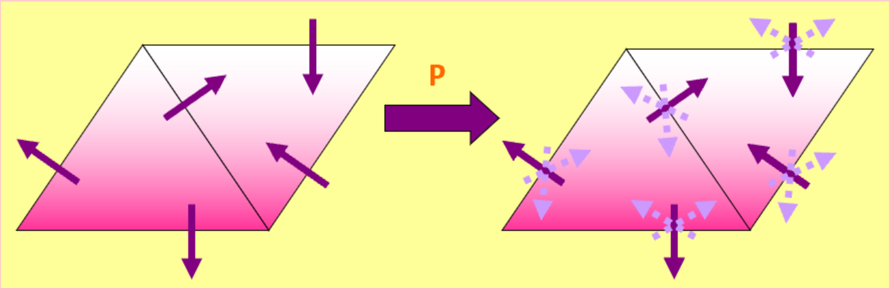

In general, magnetic order in solids becomes more stable under pressure due to increase of magnetic interaction strength.

The melting of the magnetic order and formation of the spin liquid state in compressed $YMnO_3$ is the rare example of opposite behavior, driven by geometric frustration effects

D.P.Kozlenko et al., JETP Lett. 82, 212 (2005), Phys. Rev. B 78, 054401 (2008)

Cluster reorganization in polar fullerene solutions after water addition

Collaboration: FLNP JINR Dubna – KNU, ISC NASU, Kyiv, Ukraine – RISSP Budapest, Hungary - GKSS Geesthacht, Germany

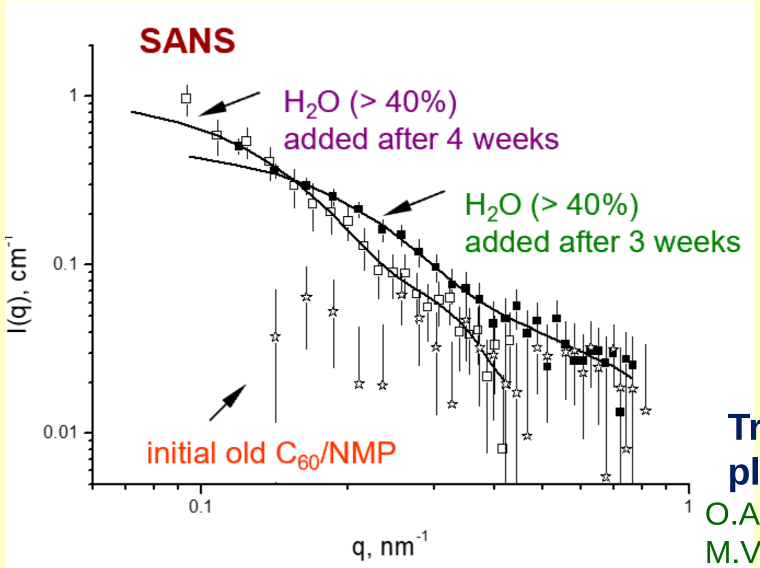

Solutions of C_{60} in N-methyl-pirrolidone (NMP)

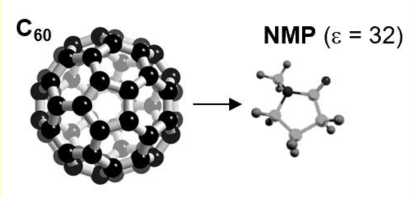

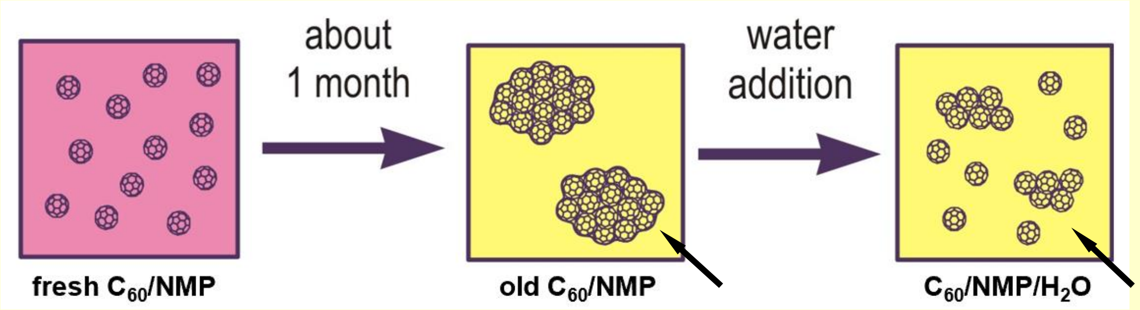

D > 100 nm

10 < D <100 nm

Transition from molecular to cluster state of C_{60} in NMP in time is revealed. Cluster stabilization takes place due to transformation of complexes C_{60}-NMP. New complexes are soluble in mixture NMP/H_2O.

O.A.Kyzyma, L.A.Bulavin, V.L.Aksenov, et al., *Fullerenes, Nanotubes and Carbon Nanostructures* (2008), O.A.Kyzyma, M.V.Korobov, M.V.Avdeev, et al., *Chem. Phys. Lett.* (2010), V.L.Aksenov, M.V.Avdeev, O.A.Kyzyma, et al., *Cryst. Rep.* (2007)

Structural Features of Magnetic Fluids

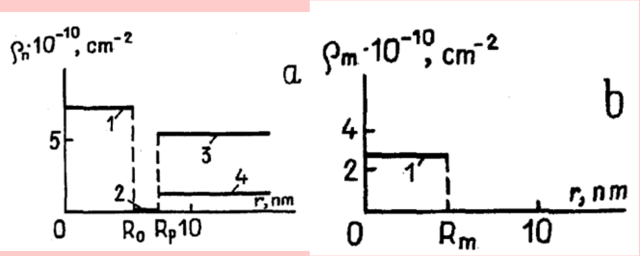

Radial distribution of nuclear (a) and magnetic (b) neutron coherent scattering density length of magnetite nanoparticles in ferrofluid.
B.Grabcev, M.Balasoiu et al., Magnetohydrodynamics 10, 156 (1994).

Magnetic nanofluids

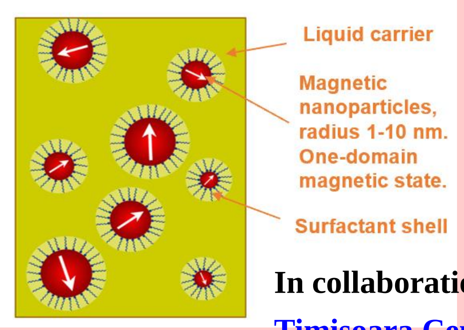

In collaboration with:

Timisoara Center, Romania
“Kurchatov Institute”, Russia
Kyiv University, Ukraine
Institute for SSP&O, Budapest, Hungary
GKSS, Geesthacht, Germany

Small-angle neutron scattering

Magnetite in cyclohexane stabilized by oleic acid (OA) and myristic acid (MA) and mixtures

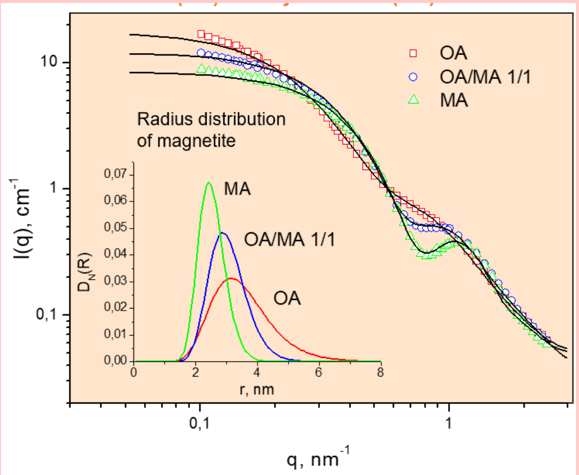

Discovered effect allows one to regulate characteristic magnetic particle radius in organic nanofluids over interval of 2.5-5 nm by using mixtures of different surfactants.

M.V.Avdeev, V.L.Aksenov, M.Balasoiu, et. al., *J. Colloids and Interface Science* (2005)

Determination of Structural Features of Dendrimers

FLNP JINR – ISPM RAS

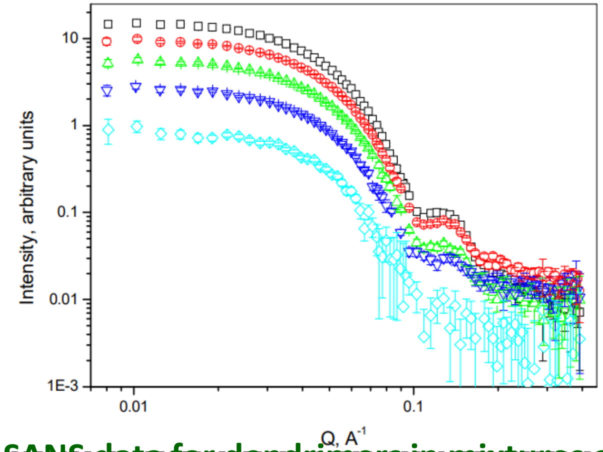

SANS data for dendrimers in mixtures of C_6H_6/C_6D_6 from bottom to top: 0/100, 75/25, 50/50, 25/75, 100/0, wt/wt %.

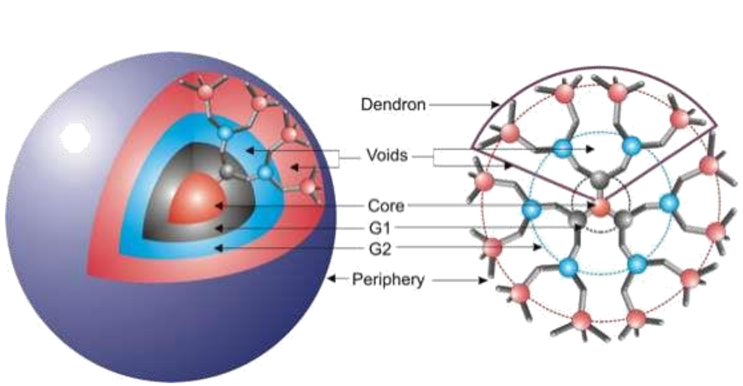

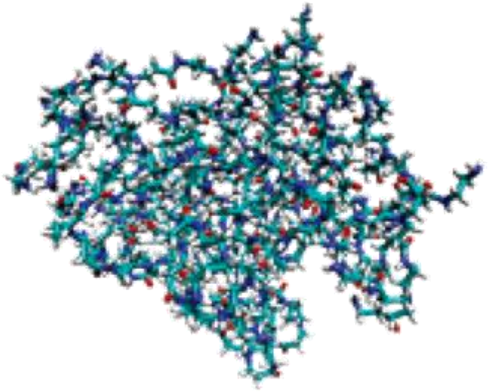

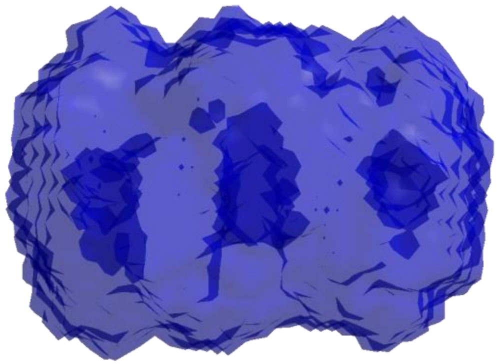

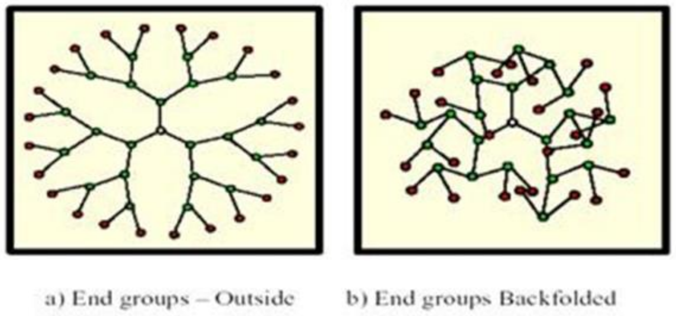

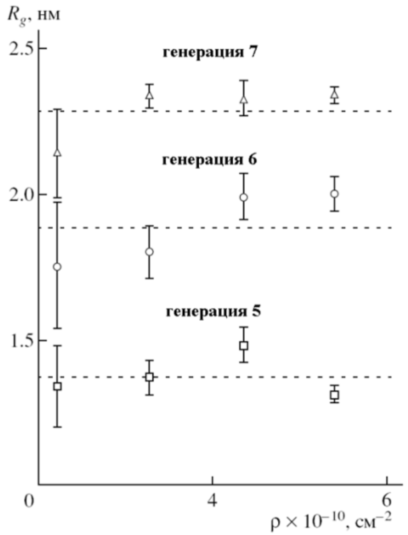

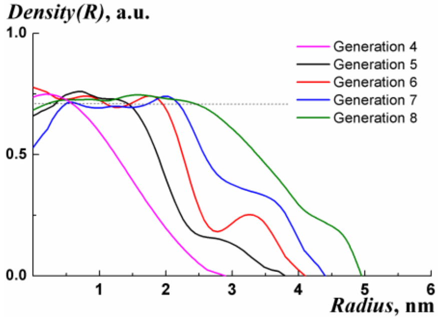

Theoretical investigation of density distribution

Kuklin A.I., Ozerin A.N., Islamov A.Kh., Rogachev A.V., Gordeliy V.I. et al., Polym. Sci. 44, 2124 (2002), J. Appl. Cryst. 36, 679 (2003), Cryst. Rep. 52, 500 (2007).

Formation of 3D structures inside mitochondria

FLNP JINR – MSU (A.N.Belozersky Research Institute)

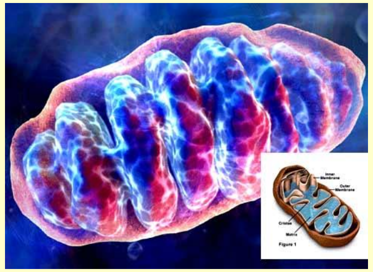

The mitochondrion is the cell power plant which produces the energy necessary to carry on all cellular processes

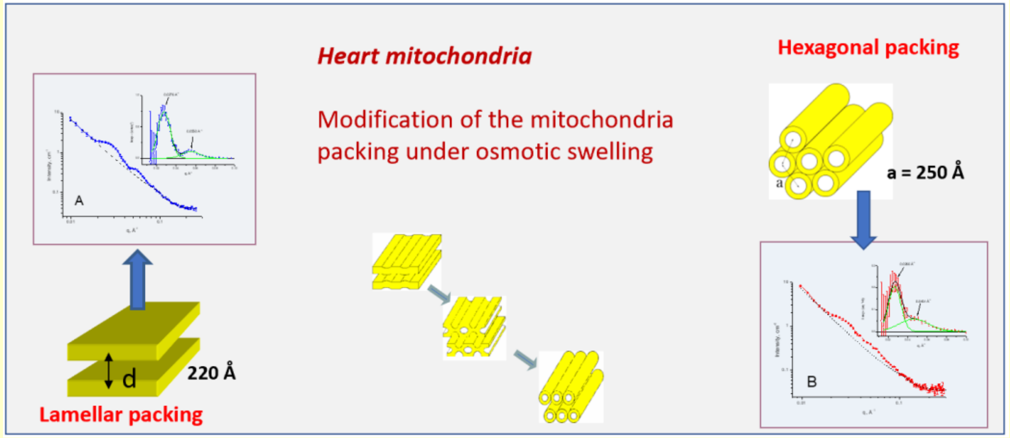

T.N.Murugova, V.I.Gordeliy, A.I.Kuklin, A.Kh.Islamov, L.S.Yaguzhinskii, Biophysics 51, 882 (2006), Cryst. Rep. 52, 521 (2007).

Studies of model stratum corneum membranes via neutron diffraction. Nanostructure, hydration, and water diffusion in real time.

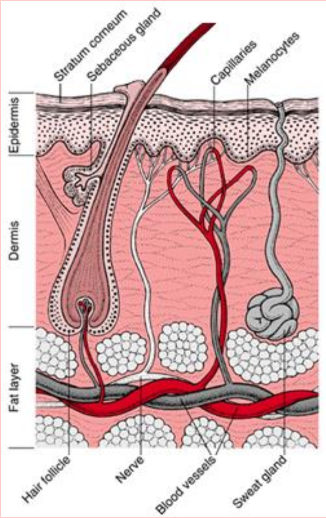

Stratum corneum (SC) is the major barrier for water and drugs penetration

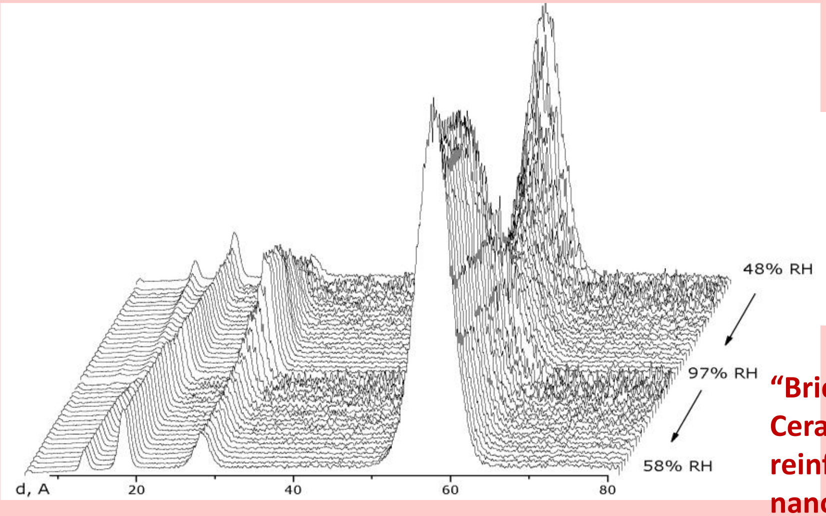

Neutron diffraction patterns measured in real time from lipid membrane at the IBR-2.

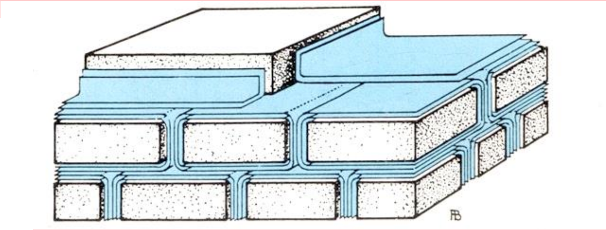

"Brick and mortar" model of the SC. Ceramide 6 molecules create armature reinforcement of the "mortar" nanostructure.

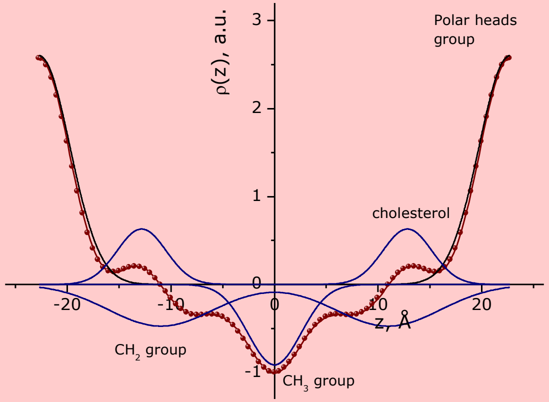

The neutron scattering length density of the CER6/Ch/PA/ChS membrane with the composition 55/25/15/5 at 60% humidity and 32C for the cases of 8, 20 and 50% D_2O content.

N. Yu. Samoylova, M. A. Kiselev, A.I.Beskrovny, A. M. Balagurov, Phys. Solid State 52, 1050 (2010)
N. Yu. Samoylova, M. A. Kiselev, A. M. Balagurov et al. *Eur. Biophys. J.* 34, 1030 (2005)

Proximity effects in superconducting/magnetic layered nanostructures

FLNP JINR – RUB (Germany), KFKI RIPNP (Hungary), ILL (France)

$V(33)/Fe(3.2)/[V(3.2)/Fe(3.2)]_{20}$

Polarized neutron spectrometer REMUR

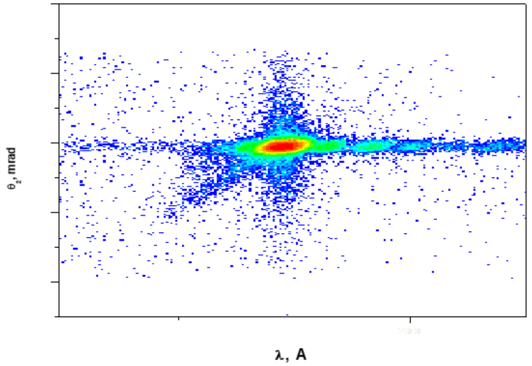

Intensity of scattered neutrons as a function of wavelength and scattering angle

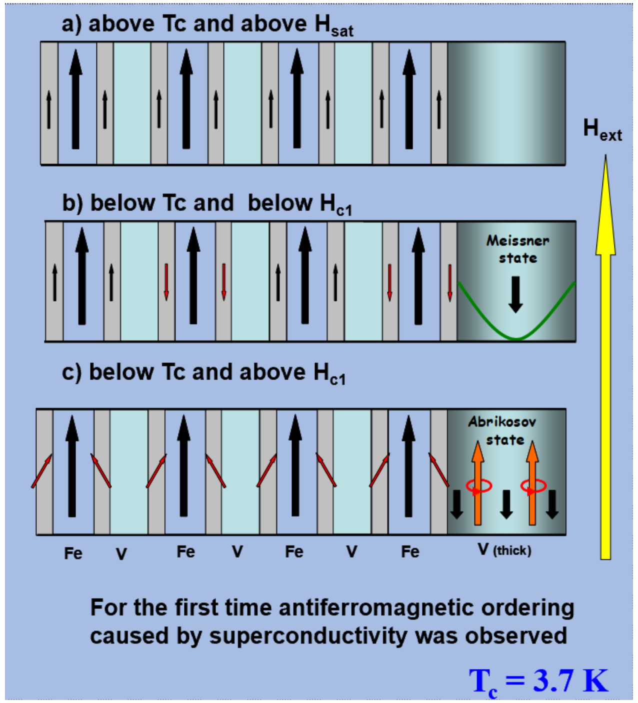

V.L.Aksenov, Yu.V.Nikitenko et al., Cryst. Rep. 52, 381 (2007)

Cu(32nm)/V(40nm)/Fe(1nm)/MgO

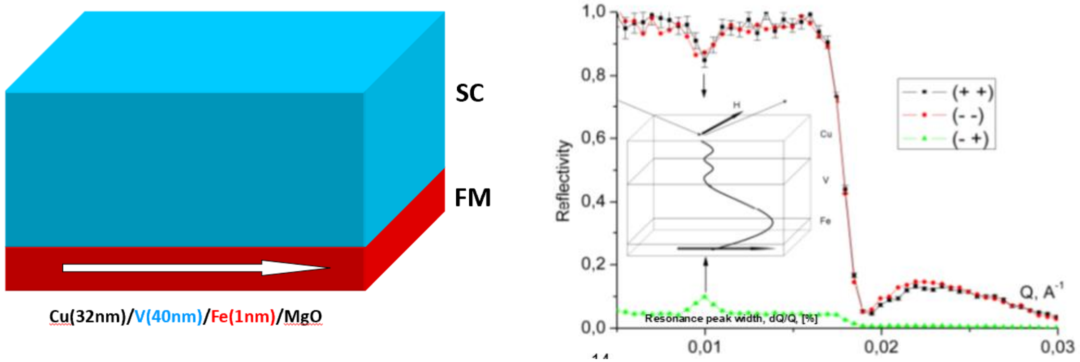

Magnetization profiles

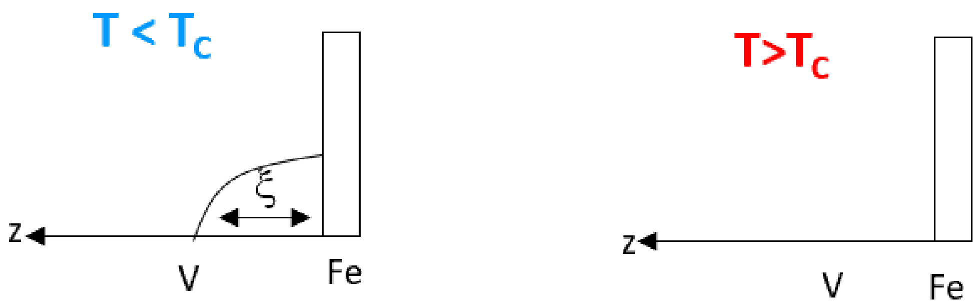

Possible Cooper pairs polarization on the interface superconductor/ferromagnet

Yu.N. Khaydukov, V.L. Aksenov, Yu.V. Nikitenko et al,
J. of Superconductivity and Novel Magnetism 24, 961 (2011)

Lattice Dynamics of Metal Trihydrates

FLNP JINR – ISSP RAS

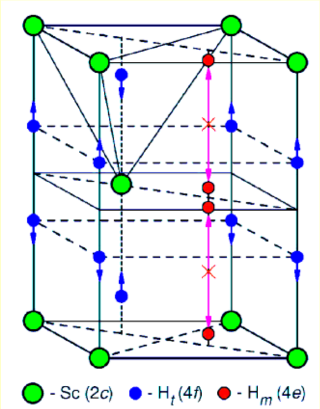

Crystal structure of scandium trihydride

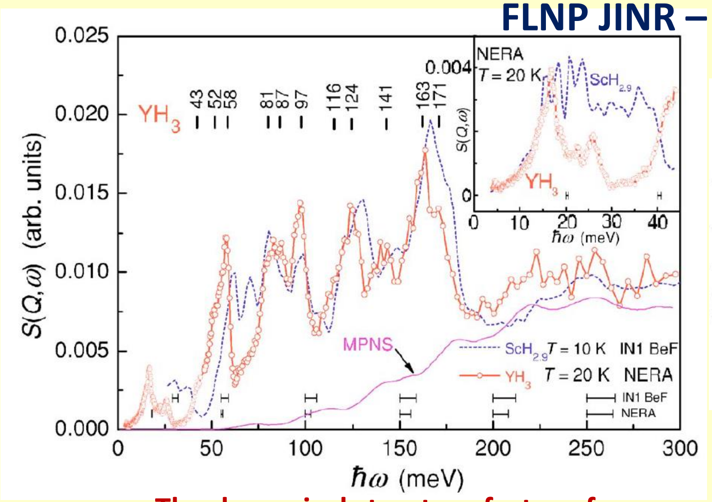

The dynamical structure factor of $ScH_{2.9}$ and YH_3 powders

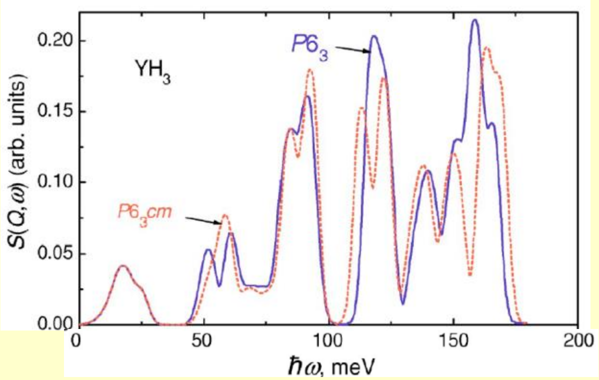

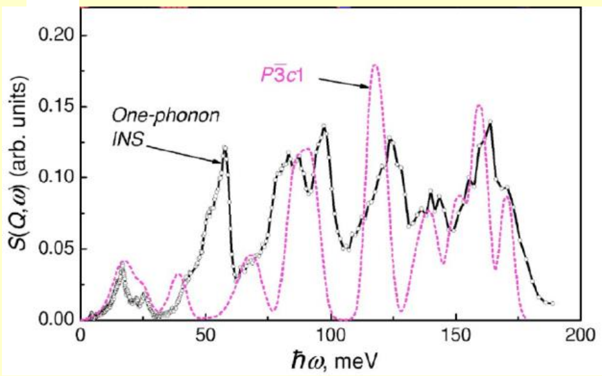

INS spectrum of YH_3 and total phonon density of states calculated for different structure models

V.E.Antonov et al., Phys Rev. B 73, 054107 (2006)

Crysal field effects in RCu_2Si_2 compounds

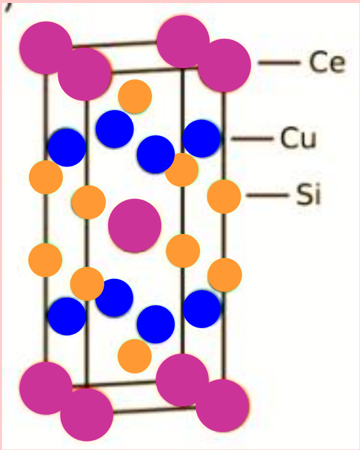

Crystal structure of RCu_2Si_2

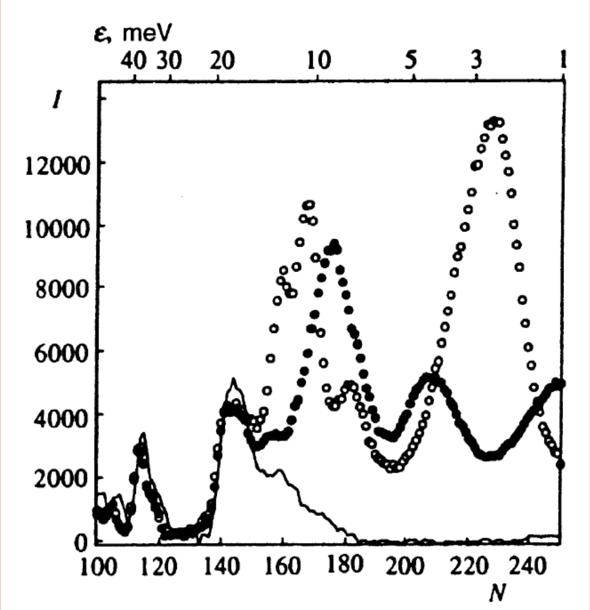

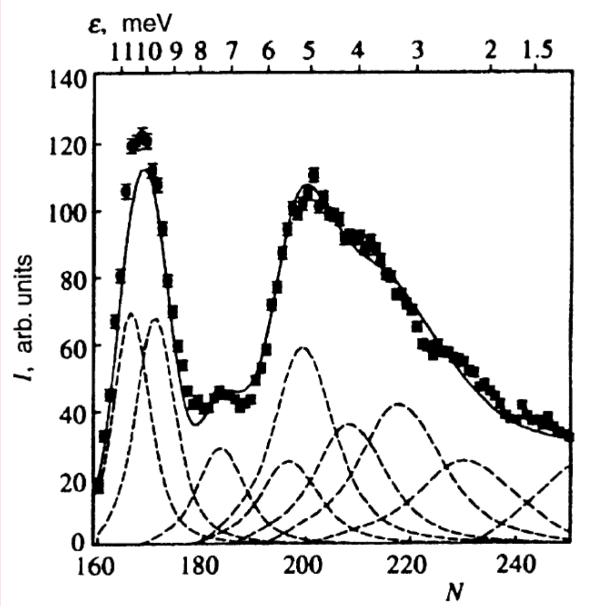

INS spectra of $PrCu_2Si_2$, $LaCu_2Si_2$ (left) and $HoCu_2Si_2$ (right) at T = 80 K

E.A.Goremychkin et al., JETP 83, 738 (1996)

Non-destructive control of residual stresses in products and materials

G.D.Bokuchava, A.M.Balagurov, V.V.Sumin, A.V.Tamonov, Yu.V.Taran


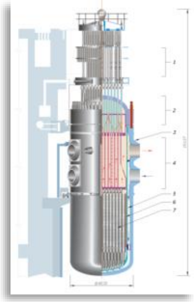

Reactor VVER 1000 for 1 GW NPP

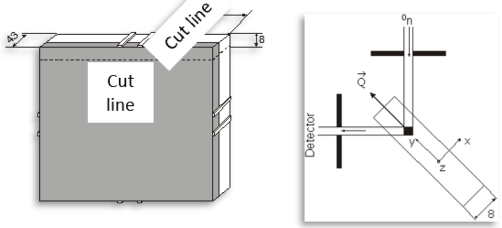

Sample part of reactor vessel and measurement scheme

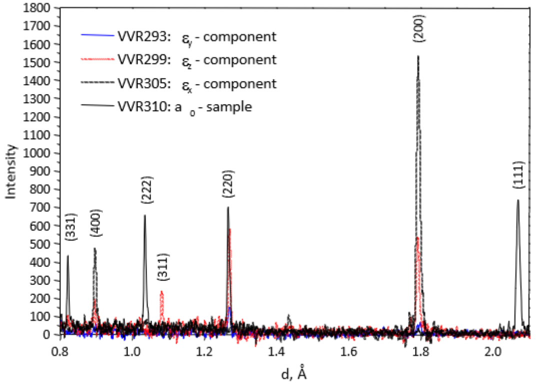

Typical neutron diffraction spectra

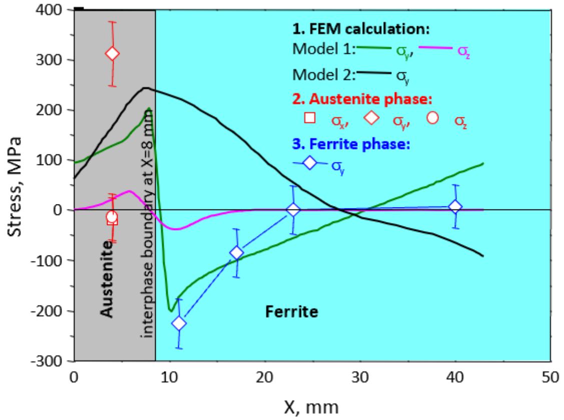

Distribution of residual stresses along the x axis

NPP based on RBMK 1000 reactor type

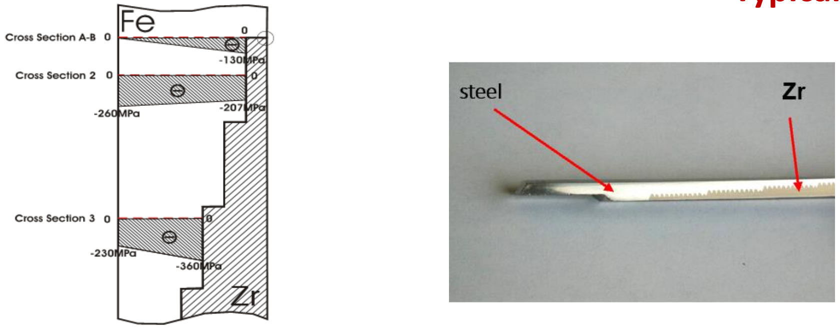

Cross-section of bimetallic steel-zirconium adapter used in RBMK reactor components and adapter wall studied in experiments

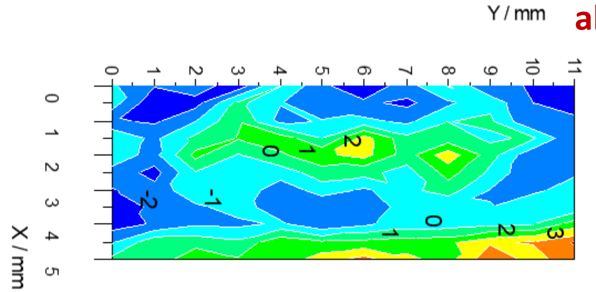

The map of axial strain tensor component in steel part of bimetallic adapter

Equipment for mining industry

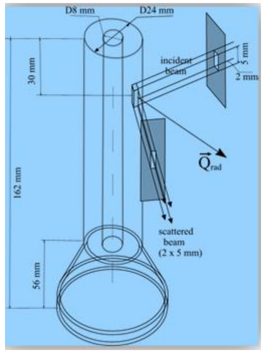

Perforator striker layout

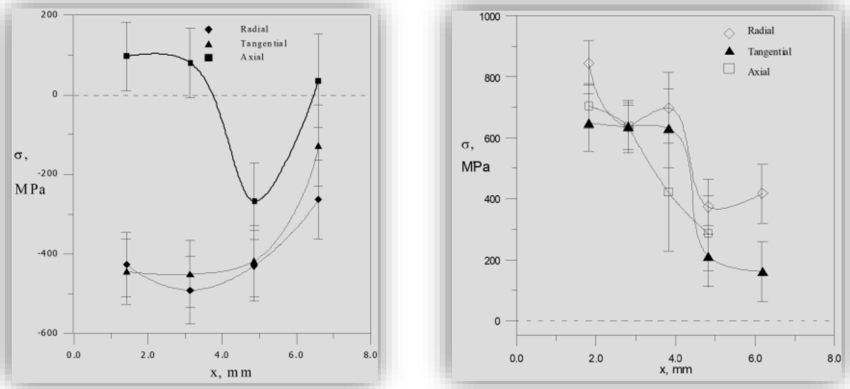

The measured residual stress distribution in the sample along radial coordinate *x*.

Texture analysis of rock samples from Kola superdeep borehole, depth 8.5-10.5 km (Russia)

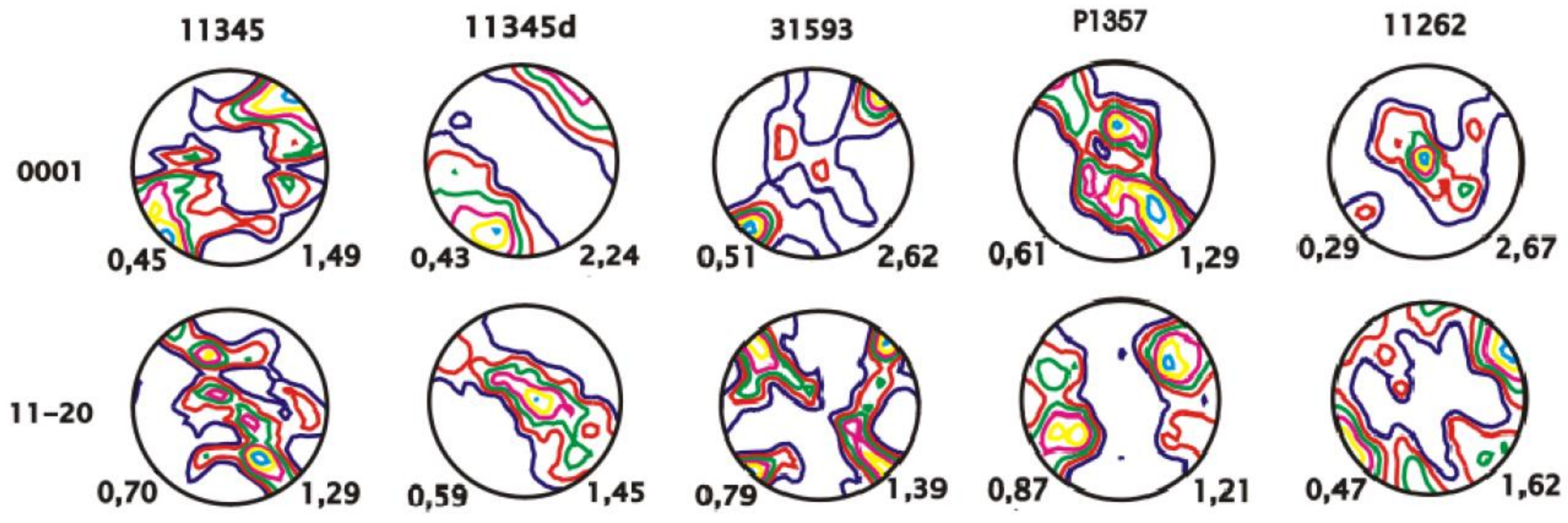

Pole figures (0001) and (11-20) of quartz in amphibolite rock samples

T.I.Ivankina, A.I.Nikitin, Izvestiya, Physics of the Solid Earth 40, 334 (2004).

SPECTROMETER COMPLEX AFTER IBR-2 MODERNIZATION (PERFORMED DURING 2007-2012) FOR CONDENSED MATTER RESEARCH

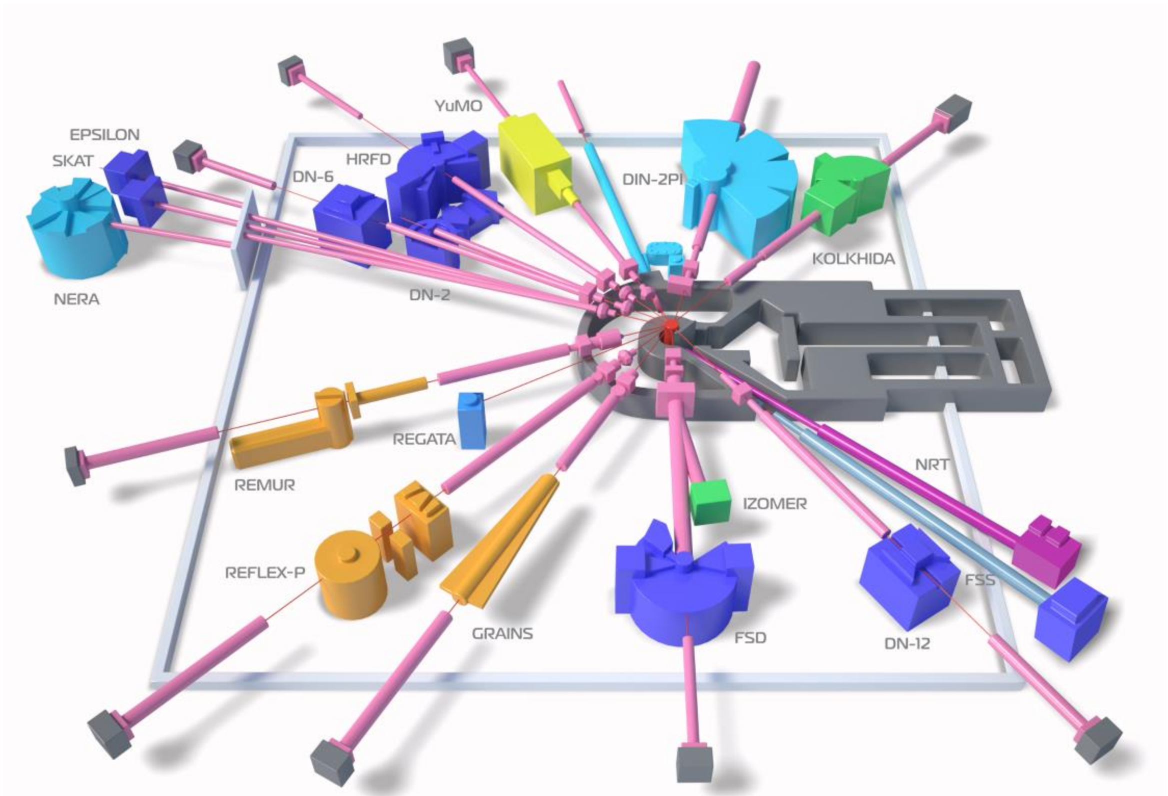

Before IBR-2 Modernization: 11 instruments in operation	→	After IBR-2 Modernization: 15 instruments in operation

New instruments have been put into operation:

- GRAINS Multifunctional Reflectometer for soft and liquid interfaces (2013) M.V.Avdeev, V.I.Bodnarchuk, V.L.Aksenov, H.Lauter;
- DN-6 Diffractometer for Studies of Microsamples at Ultrahigh Pressures (2013); D.P.Kozlenko, S.E.Kichanov, E.V.Lukin, B.N.Savenko
- NRT Neutron Radiography and Tomography Spectrometer (2013); D.P.Kozlenko, S.E.Kichanov, E.V.Lukin, B.N.Savenko, G.D.Bokuchava, A.V.Belushkin
- Fourier Stress Spectrometer (2013). G.D.Bokuchava, A.A.Kruglov, V.V.Zhuravlev

Major Upgrade:

- SKAT and Epsilon Diffractometers for Geophysical Research (2012);
- NERA Inelastic Neutron Scattering Spectrometer (2012);
- Reconstruction of DN-2 into Real Time Diffractometer RTD (2016);
- High Resolution Fourier Diffractometer (2016);
- REMUR (Development of equipment for Isotope Identified Neutron Reflectometry, 2018).

USER PROGRAMME AT THE SPECTROMETER COMPLEX OF MODERNIZED IBR-2 SINCE 2012

Access to spectrometers complex of IBR-2M for interested researchers (including JINR, JINR member states and non-member states) is based on selection process by Expert Committees

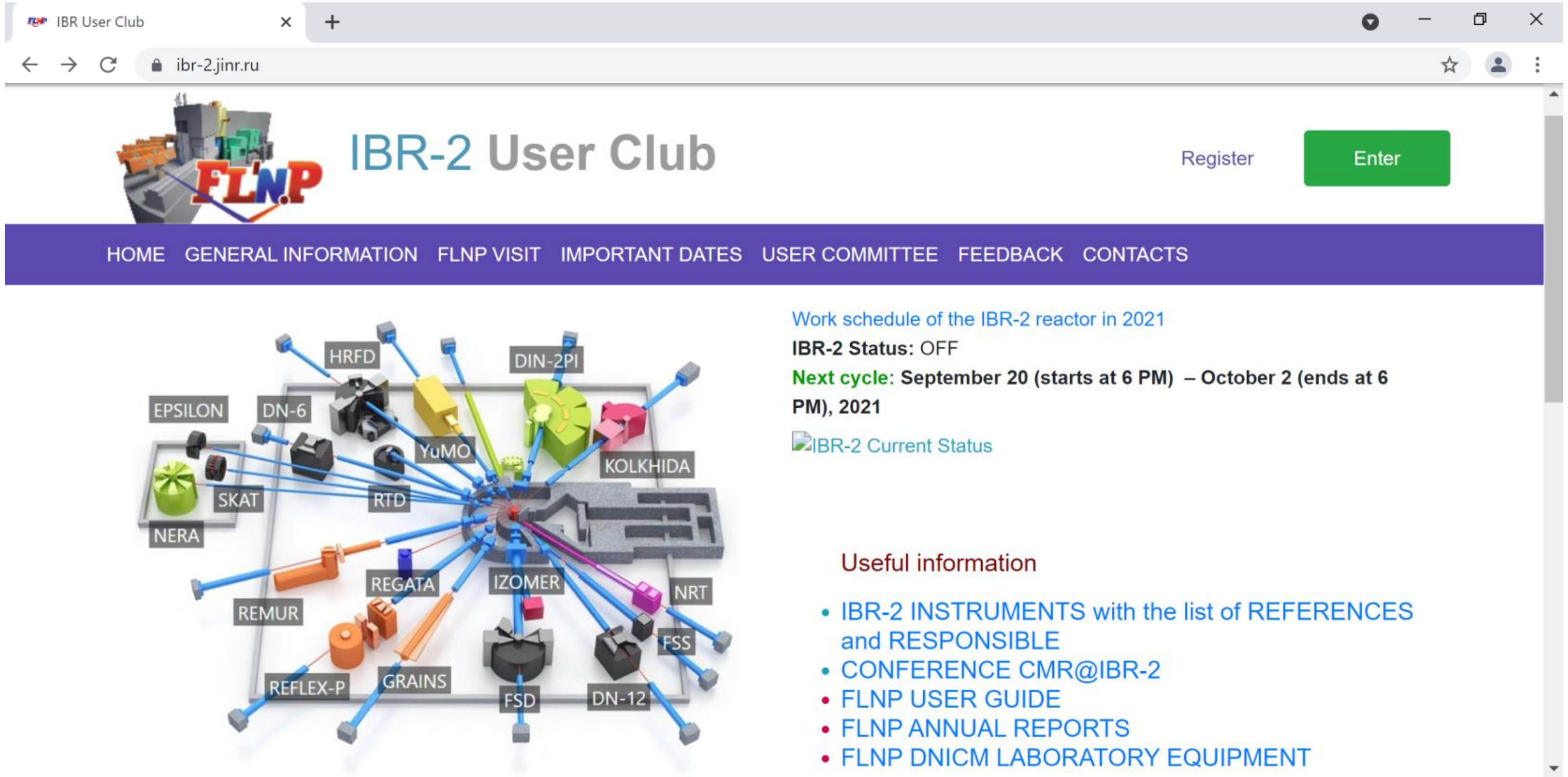

From 163 proposals submitted for the 1st call in 2012 to 297 proposals received in 2021

Main research directions :

1. Condensed Matter Physics and Materials Science,

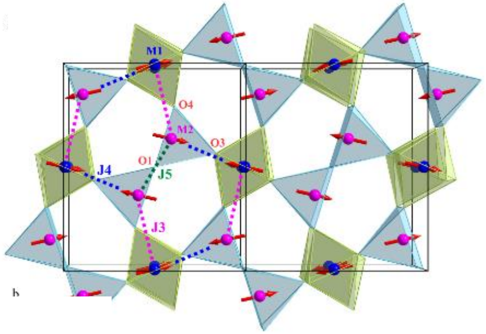

2. Physics of Nanosystems and Nanoscale Phenomena,

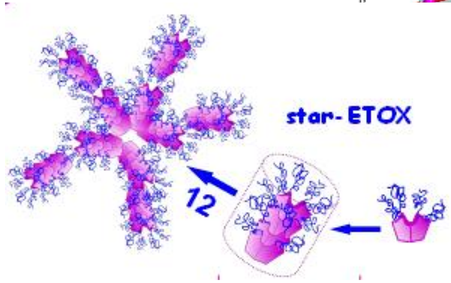

3. Physics of Complex Liquids and Polymers,

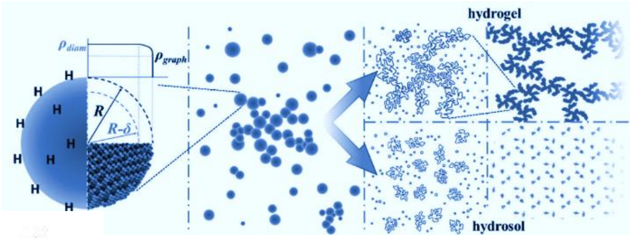

4. Biophysics and Pharmacology,

5. Applied Materials and Engineering Sciences.

Structural and Magnetic Phenomena in Low Dimensional van der Waals Magnetic Materials

Spin-induced negative thermal expansion in $CrBr_3$

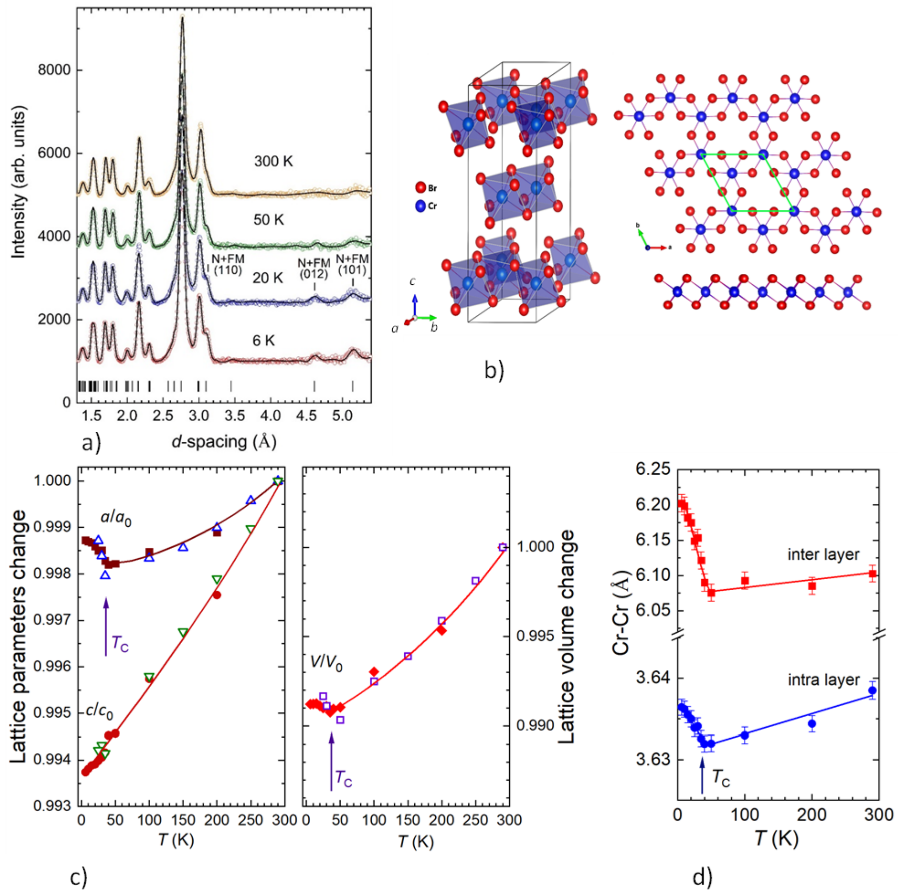

a) Neutron diffraction spectra of $CrBr_3$, measured at various temperatures. b) Crystal structure of $CrBr_3$ and layout of van der Waals layers. c) Temperature dependences of lattice parameters and unit cell volume. d) Temperature dependences of intra-layer and inter-layer Cr-Cr distances.

Transition from 2D to 3D Magnetism in $FePS_3$

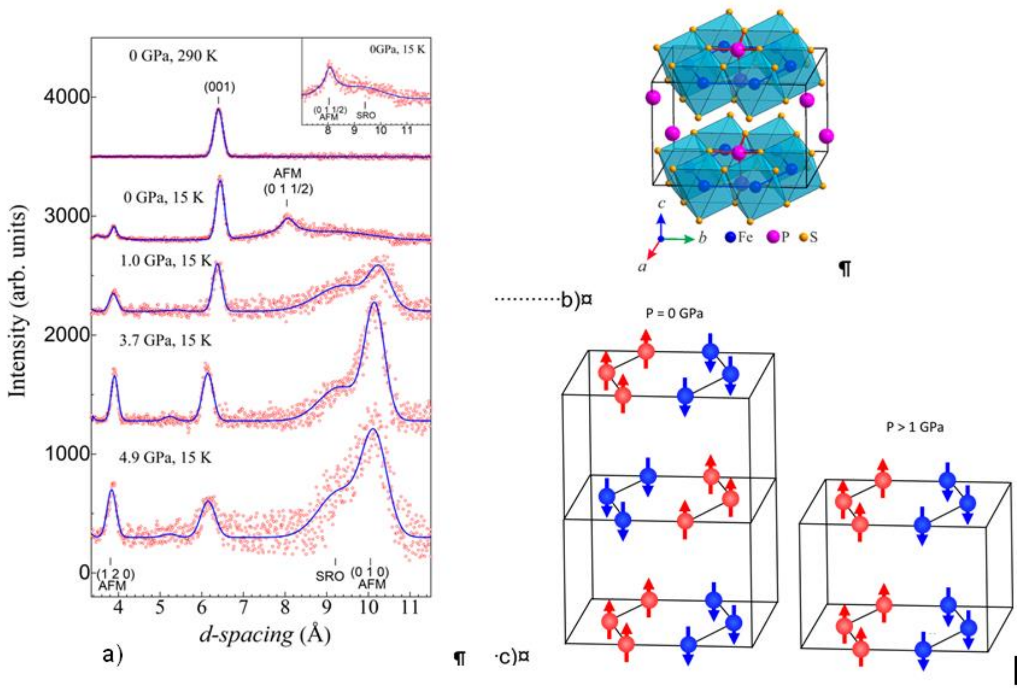

(a) Neutron diffraction spectra of $FePS_3$, measured at various pressures and temperatures. (b) Crystal structure of $FePS_3$. (c) Magnetic structure of $FePS_3$ at ambient and high pressures.

D.P.Kozlenko et al., npj Quantum materials 6: 19 (2021), (Q1, IF = 6.856)
M.J.Coak,..D.P.Kozlenko et al., Physical Review X, 11 (2021) 011024 (Q1, IF = 14.417)
N.T.Dang, D.P.Kozlenko et al., Advanced Science 2206842 (2023) (Q1, IF = 17.52)

STUDIES OF FUNCTIONAL MAGNETIC MATERIALS AT ULTRAHIGH PRESSURES

Magnetite Fe_3O_4 demonstrates pressure-induced anomalous behavior of magnetic and electronic properties of in vicinity of the structural phase transition, occurring at *P* ~ 25-30 GPa

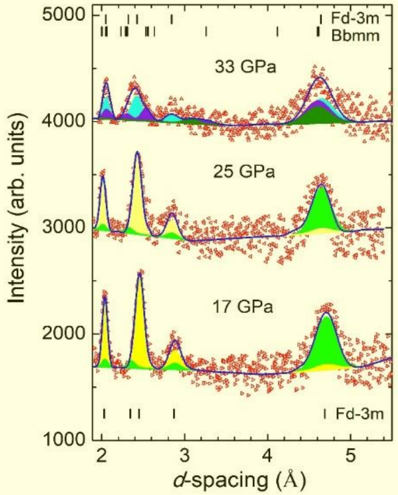

Neutron diffraction patterns measured at pressures up to 35 GPa

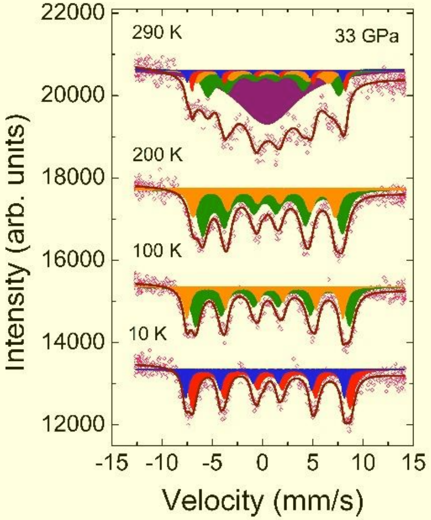

Synchrotron Moessbauer spectra of ^{57}Fe-enriched magnetite measured at 33 GPa and different T

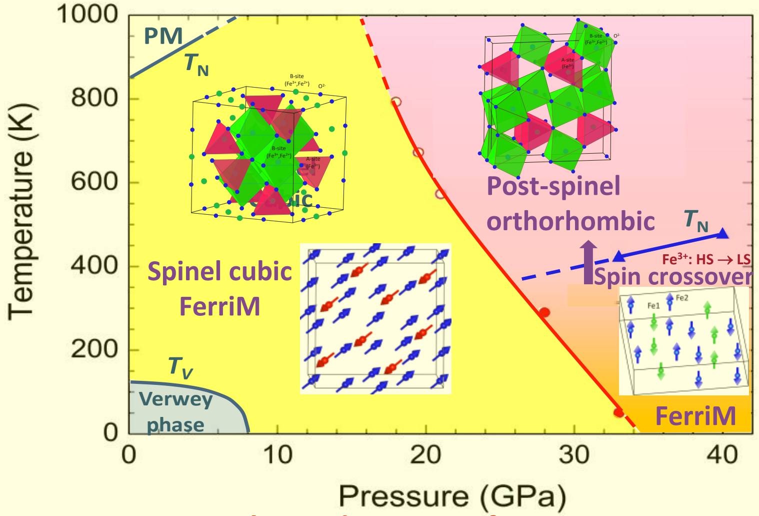

P-T phase diagram of magnetite

D.P.Kozlenko et al., Scientific Reports 9, 4464 (2019)

Suppression of orbital and antiferromagnetic order in $LaMnO_3$ at high pressure

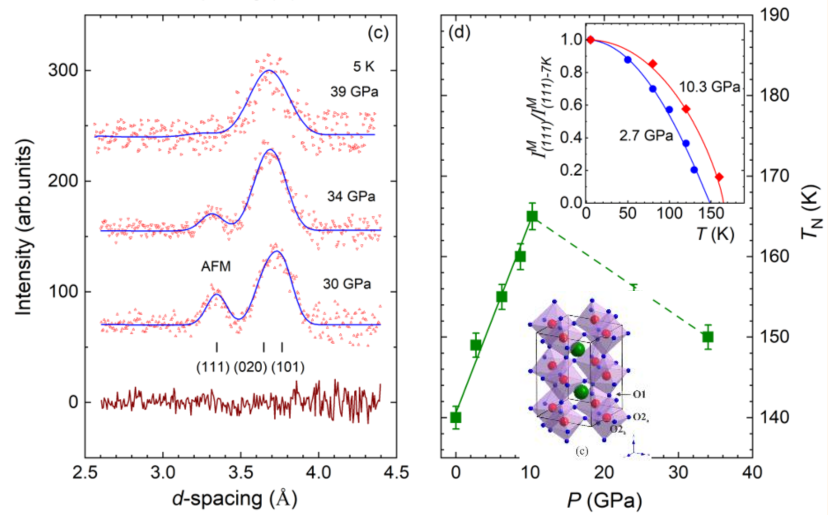

Neutron diffraction patterns of $LaMnO_3$ at high pressures up to 39 GPa and pressure dependence of Neel temperature

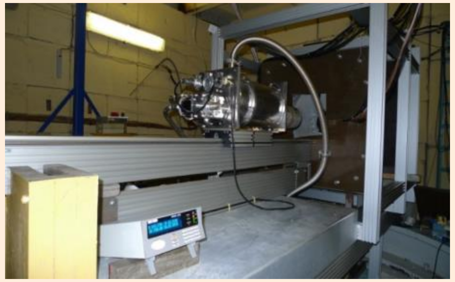

DN-6 Diffractometer

D.P.Kozlenko et al., Phys. Rev. B 107 144426 (2023)

Magnetic structure and novel type of the charge ordering state in iron oxide Fe_4O_5 involving competing dimer and trimer formation

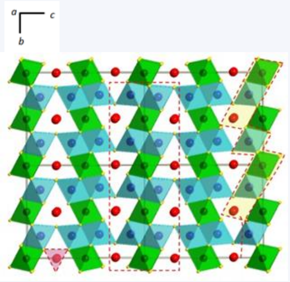

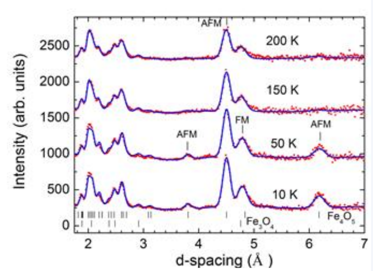

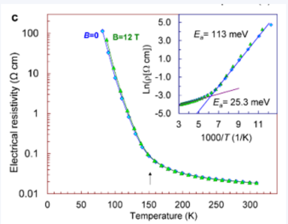

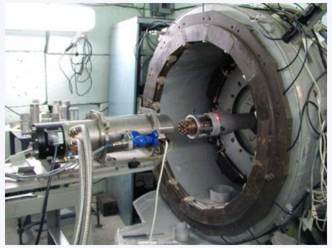

DN-12 Diffractometer

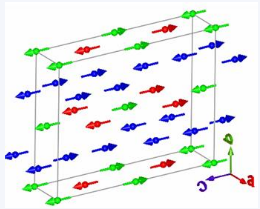

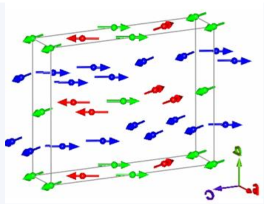

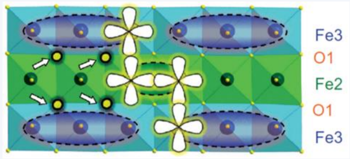

Crystal structure of Fe_4O_5, neutron diffraction patterns, measured at different temperatures, resistivity, magnetic structures at *T* = 150 and 10 K.

S.V.Ovsyannikov,.., D.P.Kozlenko, et al., Nature Chemistry 8, 501 (2016)

STUDIES OF MATERIALS FOR COMPACT ELECTRIC CURRENT SOURCES

Real-time studies of structural changes in Li-based accumulators during charging and discharging processes (HRFD)

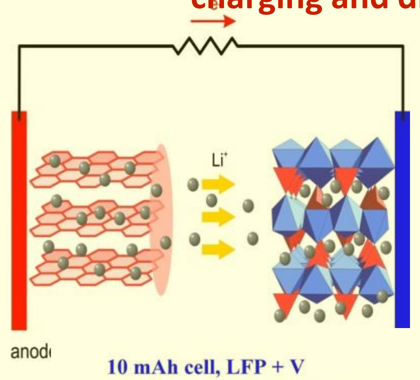

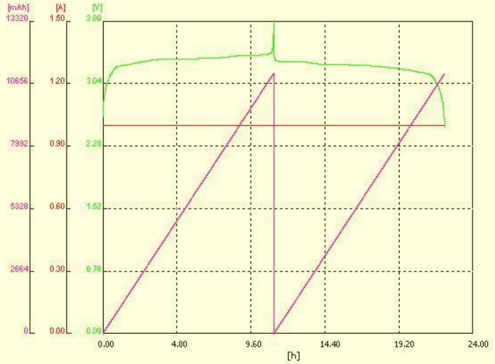

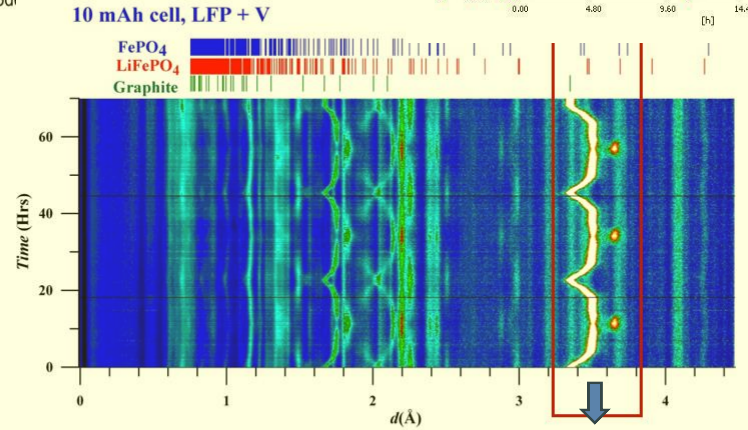

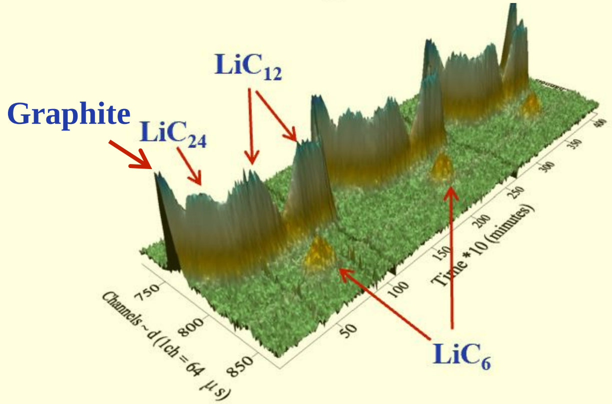

Evolution of neutron diffraction patterns of Li accumulator with $LiFePO_4$+*x*V working substance during three cycles of charging-discharging *I.A.Bobrikov et al., J. Power Sources (2014)*

Effect of non-electroactive additives on electrochemical interfaces by neutron reflectometry (GRAINS)

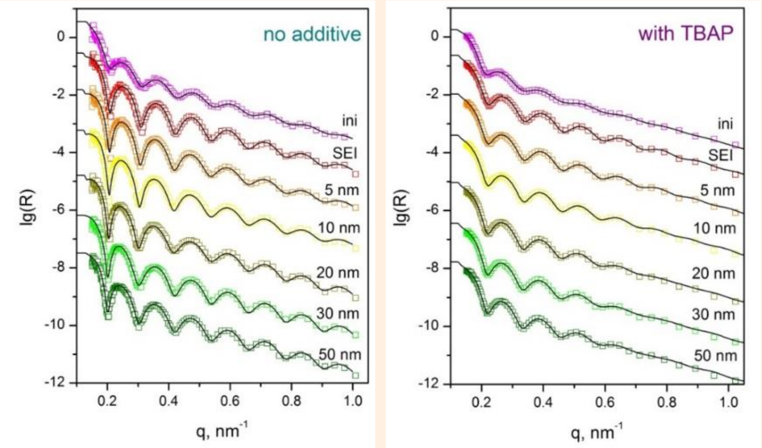

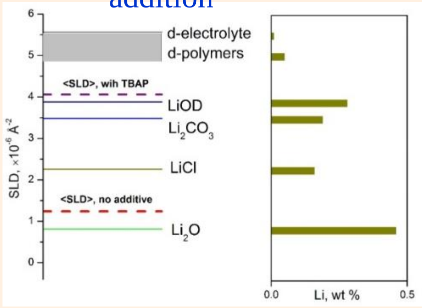

NR Study of TBAP Effect on Li Plating
M.V.Avdeev et al., Appl. Surf. Sci. (2019)

Structure of Li-deposition Layer

Nanoscale effects in Li-air batteries by SANS (YuMO)

Filling of porous carbon cathode by Li_2O_2

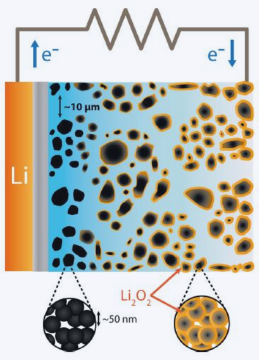

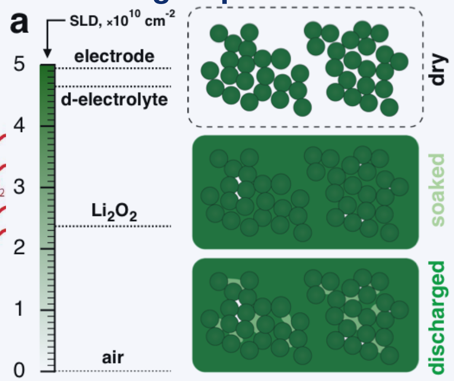

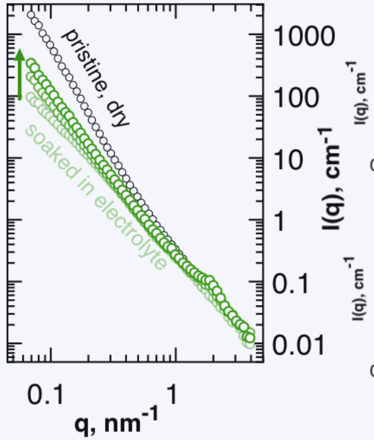

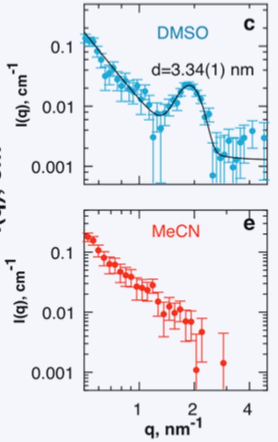

Formation of Li_2O_2 mesocrystals

T.K. Zakharchenko et al. Nanoscale (2019)

STRUCTURAL FEATURES AND PHASE TRANSITIONS IN Fe-Ga GIANT MAGNETOSTRICTIVE ALLOYS

JINR – NUST MISIS

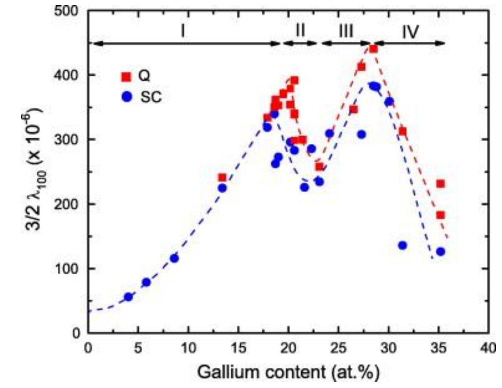

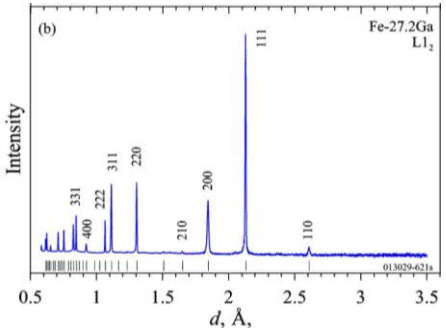

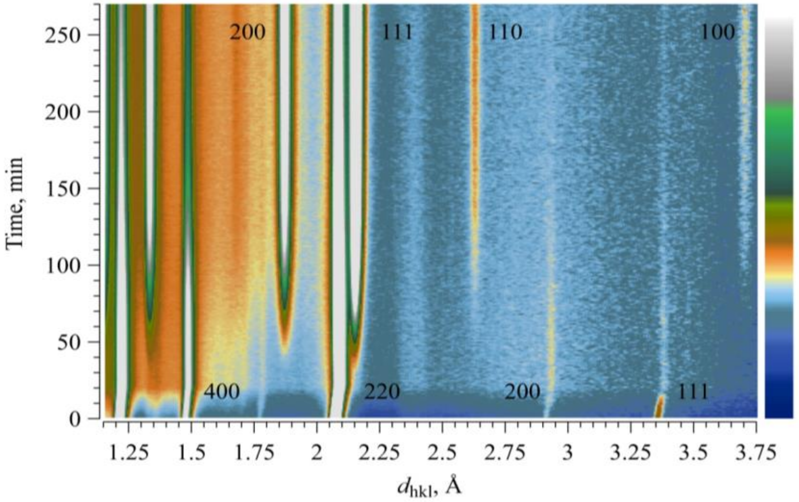

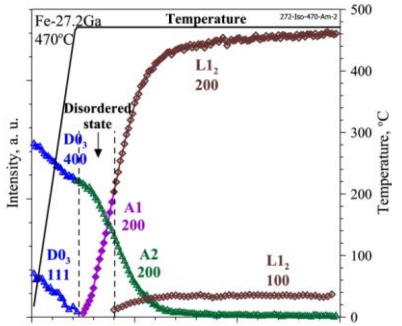

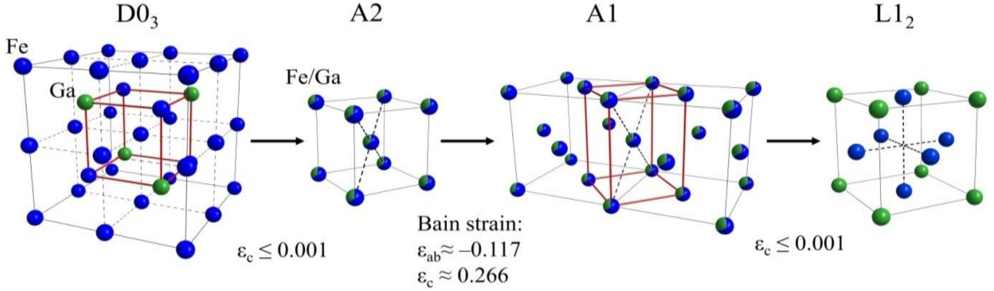

Structural phase transitions in Fe-Ga alloys on isothermal exposure

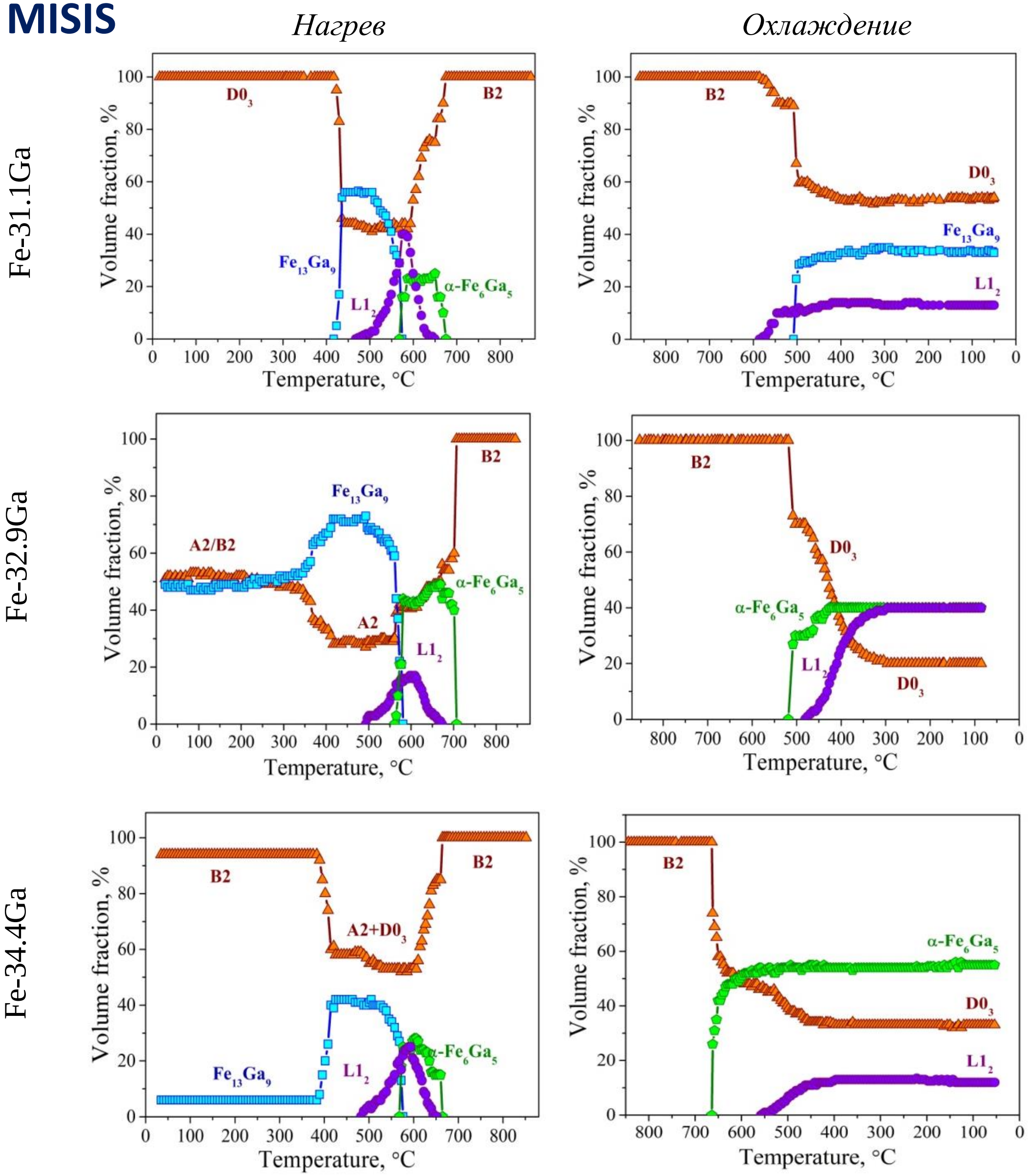

Temperature evolution of structural phases in Fe-Ga alloys

A.M. Balagurov et al., Acta Cryst. B 75, 1024 (2019)

T.N.Vershinina et al., J. of Alloys and Comp. (2022)

Magnetic nanoparticle assembling induced by non-homogeneous magnetic field at interface by neutron reflectometry

(FLNP JINR – KNU – IEP SAS)

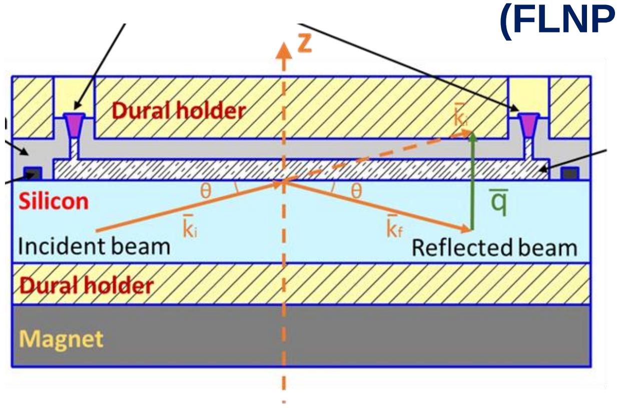

Principal scheme of a sample cell for NR experiments on the ferrofluid/silicon interface under an external magnetic field

Reflectivity curves

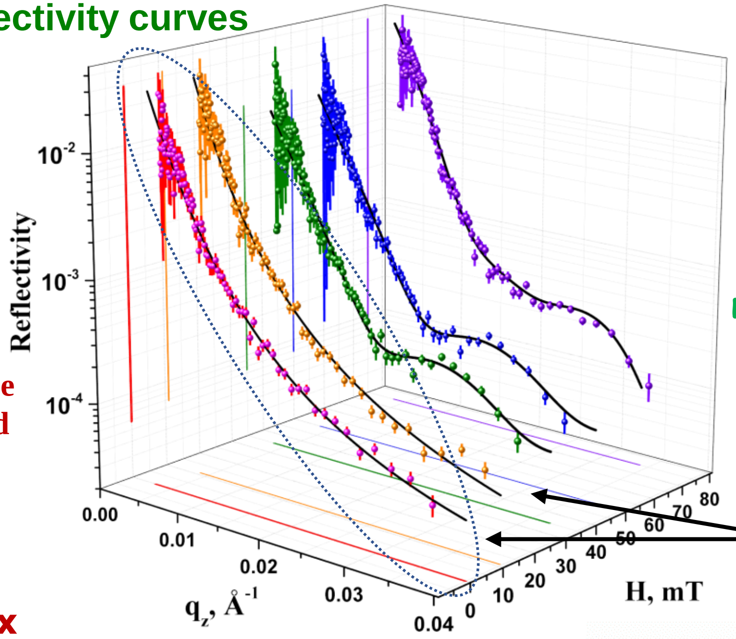

no visible structural ordering of MNPs at near-interface region at low magnetic field

zero and weak magnetic fields

Reflectivity curves

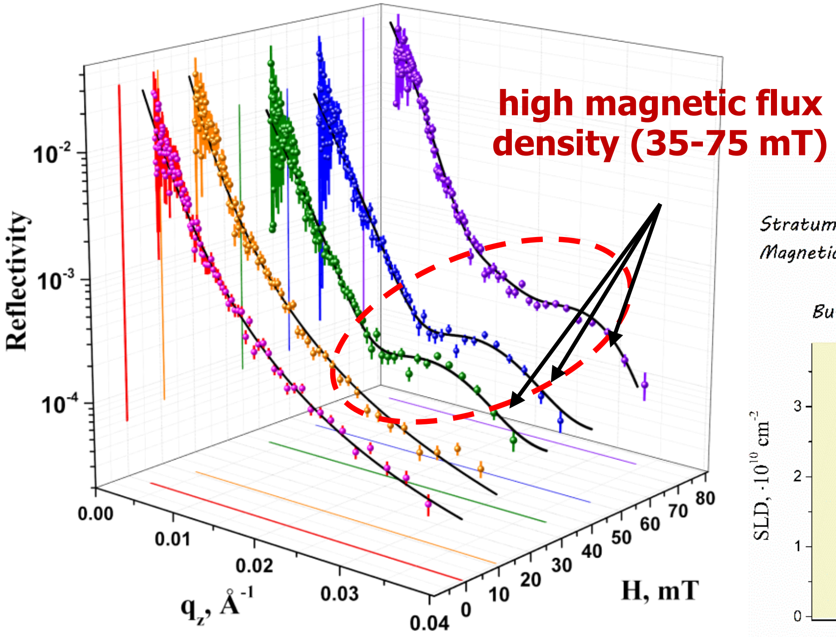

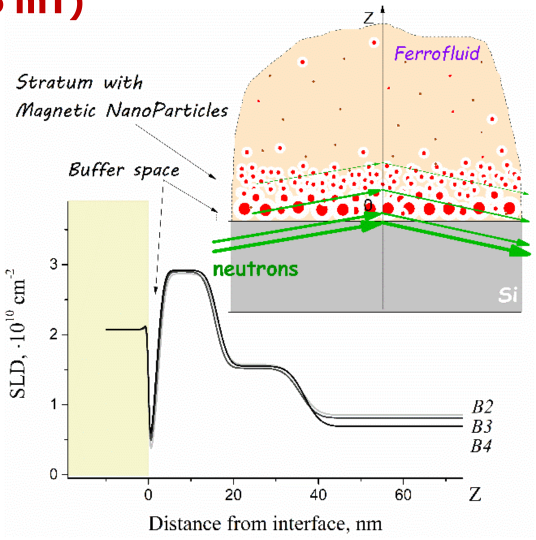

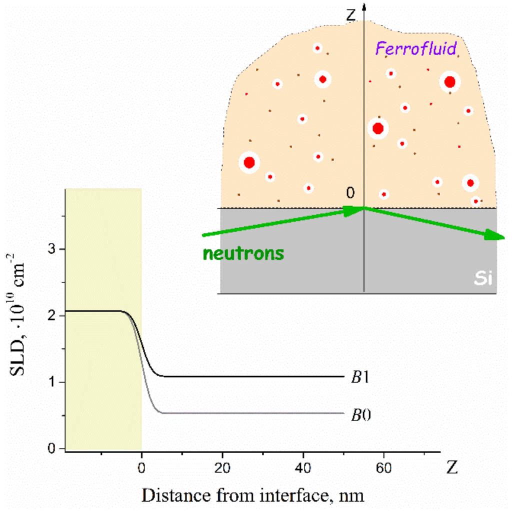

A.V.Nagornyi, V.I.Petrenko, M.Rajnak, et al. *Appl. Surf. Sci.* 473, 912 (2019).

Effect of Magnetism on Superconductivity in Nb/Gd/Nb Trilayers

FLNP JINR – IMP Ural Branch RAS – MPI FKF (Germany)

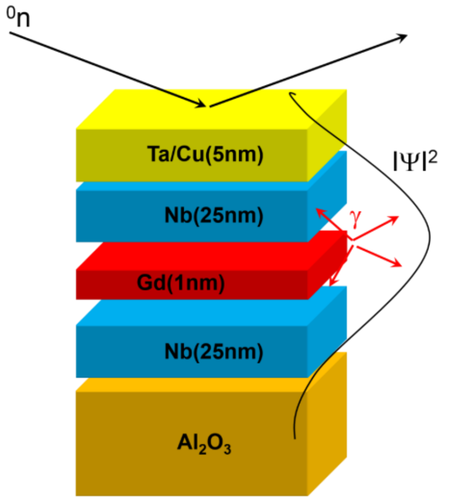

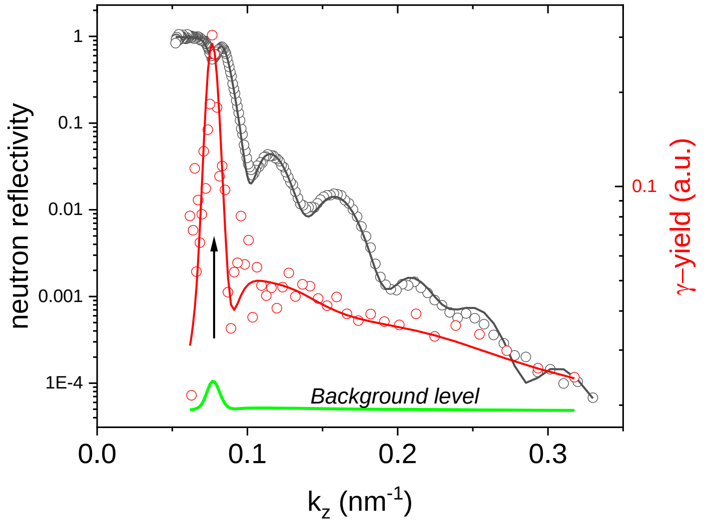

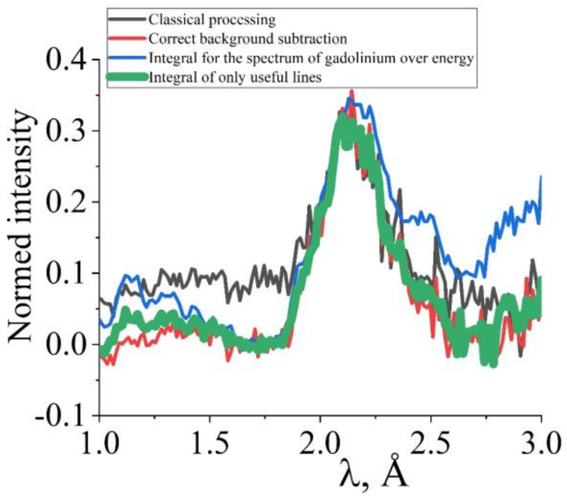

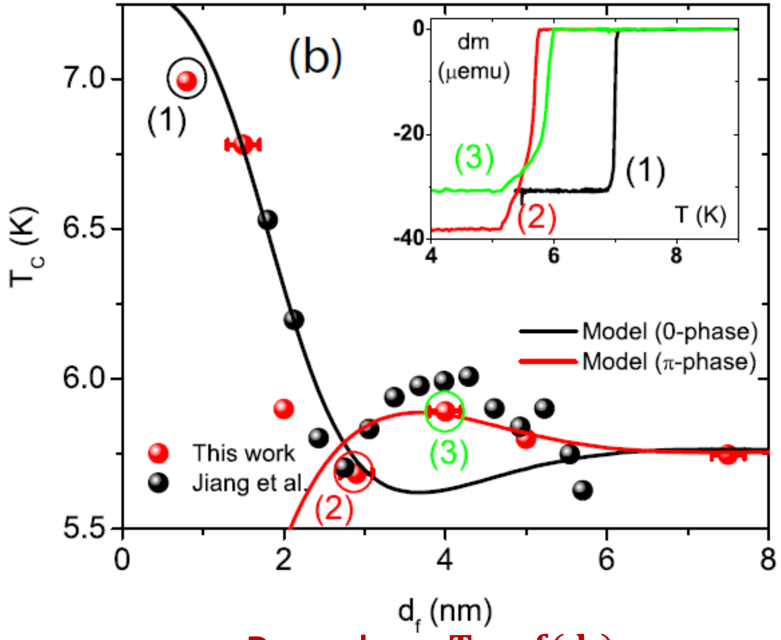

Dependence $T_c = f(d_f)$

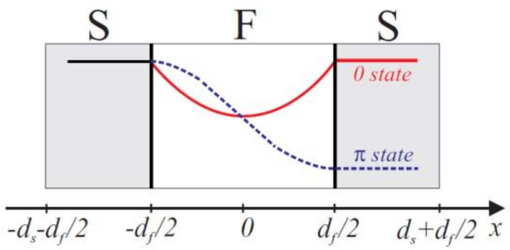

$$\xi_F = 4\ nm$$

$$d_F < \xi_F$$

- **Structures Nb(25nm)/Gd(d_f)/Nb(25nm) were investigated**
- **Observed reducing of T_c with increasing of magnetic moment**
- **Superconducting coherent length in gadolinium $\xi_F = 4$ nm**

Yu.N.Khaydukov et al., Phys. Rev. B, 97, 144511 (2018)

A study of vibrational dynamics of glass-forming single-phenyl-ring polar alcohols

JINR – INP Krakow (Poland)

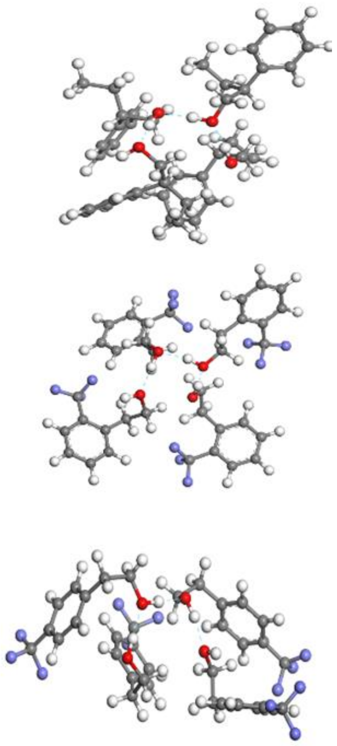

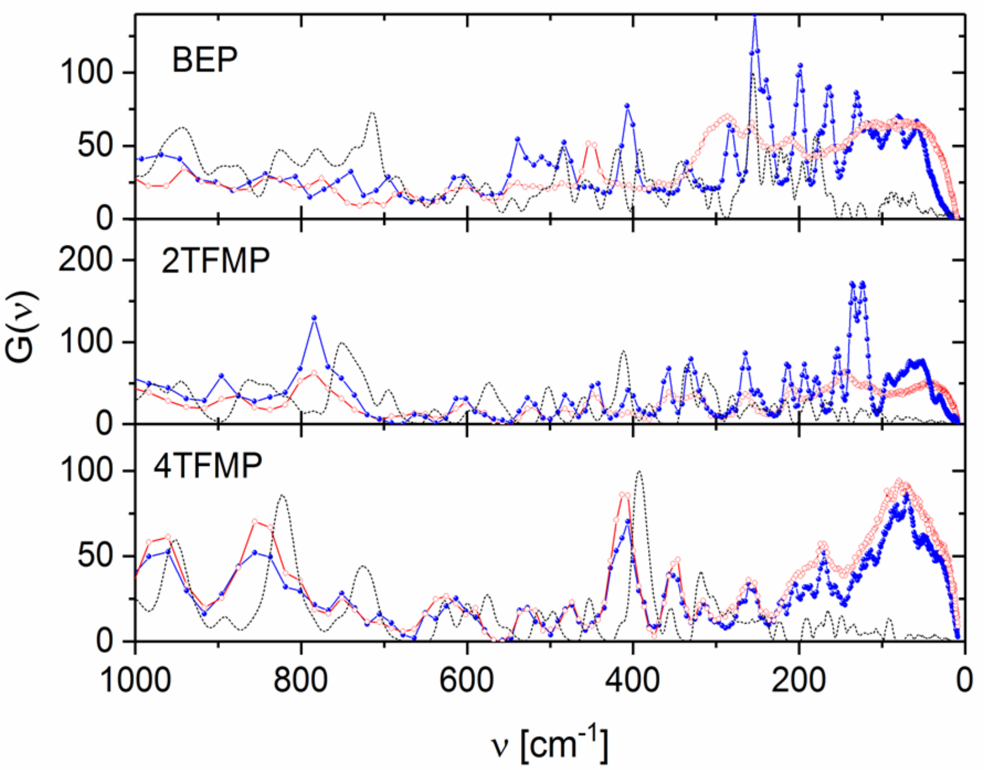

Schematic representation of the crystal structure (left) and generalized density of vibrational states of solid phases, i.e., crystalline (blue) and glass of isotropic liquid (red) at 5 K for *2-Phenylbutan-1-ol (BEP), 2-(Trifluoromethyl)phenethyl Alcohol (2TFMP) and 4-(Trifluoromethyl)phenethyl Alcohol (4TFMP)* (right). Dashed lines correspond to results of theoretical calculation for tetramer clusters

E. Juszyńska-Gałązka et al., Phase Transitions 91, 170 (2018)

STRUCTURAL MODICIATIONS IN LIPID OBJECTS AT PRESENCE OF AMYLOID-BETA PEPTIDE

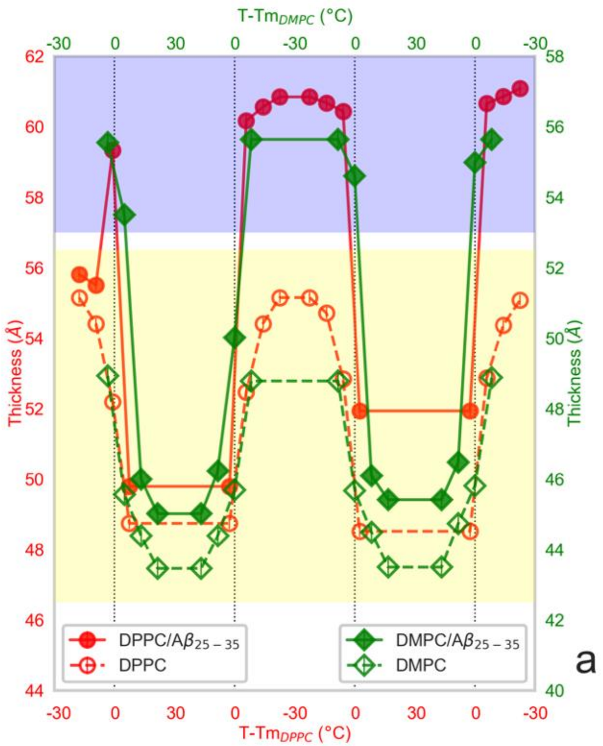

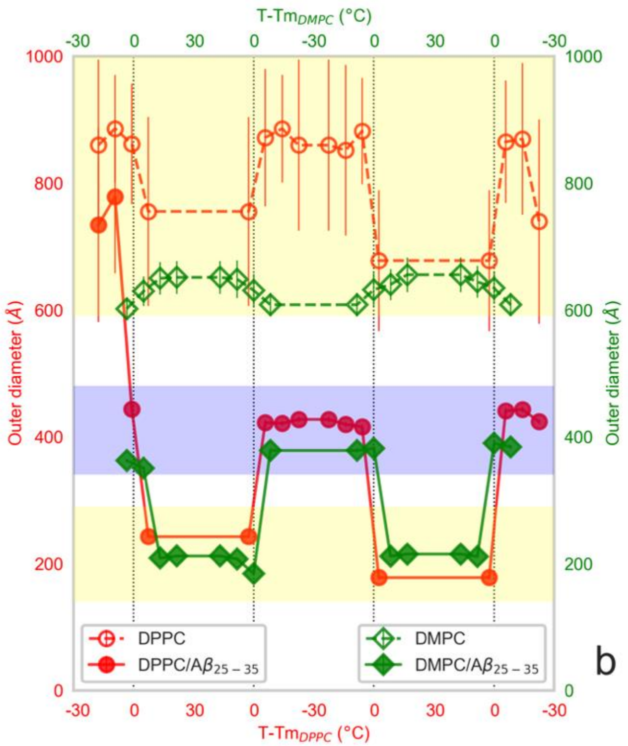

Thickness variation of the model membrane (a) and aggregate sizes (b) depending on temperature shift relatively to the main phase transition for DMPS ДМФХ (green rhombuses) and DPPC (red circles) with and without addition of amyloid-beta peptide.

O.I.Ivankov et al., Scientific Reports 11, 21990 (2021)

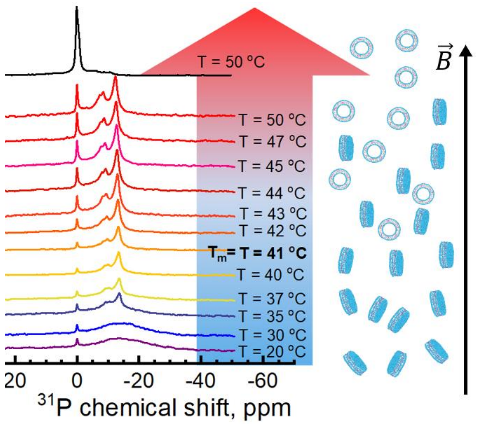

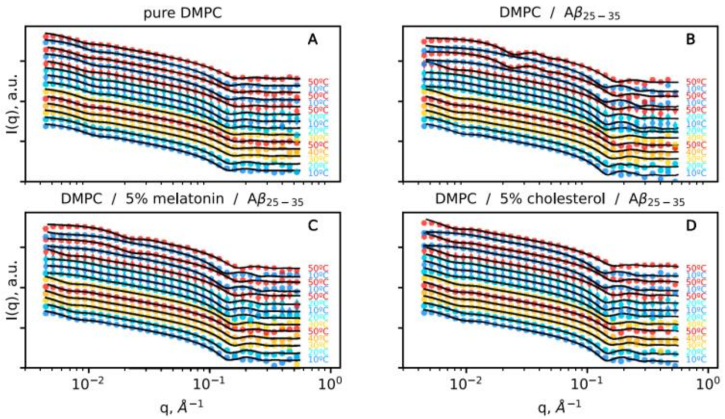

^{31}P NMR Spectra

SANS curves

Saturated phospholipids + Aβ(25-35) peptides

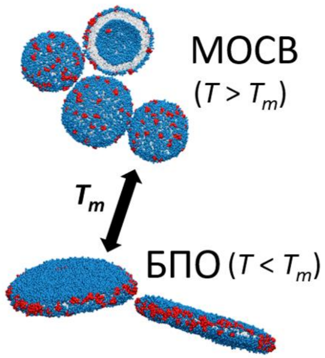

Aβ(25-35) peptides form predominantly unsaturated disordered structures

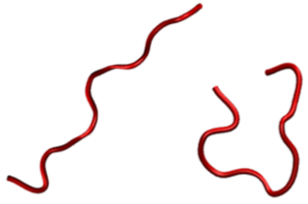

Random coils **β turns**

S.A.Kurakin et al., Biochimica et Biophysica Acta – Biomembranes, 1866, 184237 (2024)
O.I.Ivankov et al., Scientific Reports 11, 21990 (2021)

Prediction of Microscopic Residual Stresses using Genetic Programming (GP)

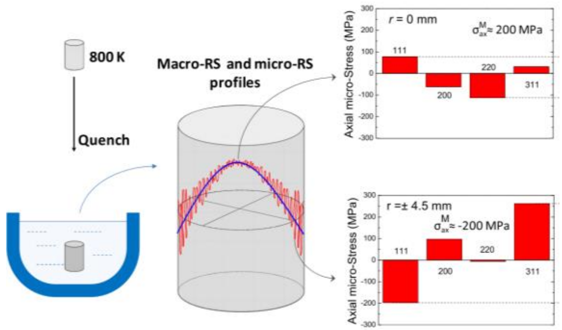

Profiles of axial residual macro- (blue) and microstresses (red)

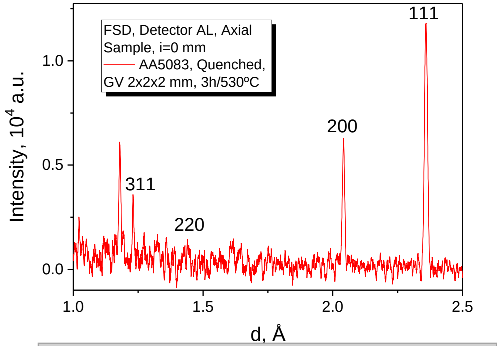

Neutron diffraction pattern

Collaboration:
- FLNP JINR (Dubna, Russia),
- CENIM (Madrid, Spain),
- BAM (Berlin, Germany)
- Research Centre Řež (Řež, Czech Rep.)
- Uni. of Applied Sciences Upper Austria (Hagenberg, Austria)

Fourier Stress Diffractometer (FSD) @ IBR-2 reactor

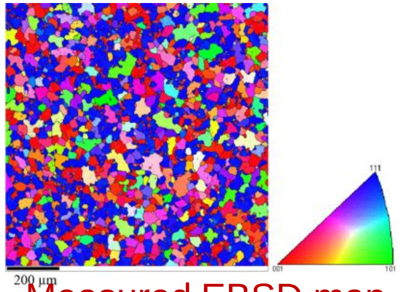

Measured EBSD map

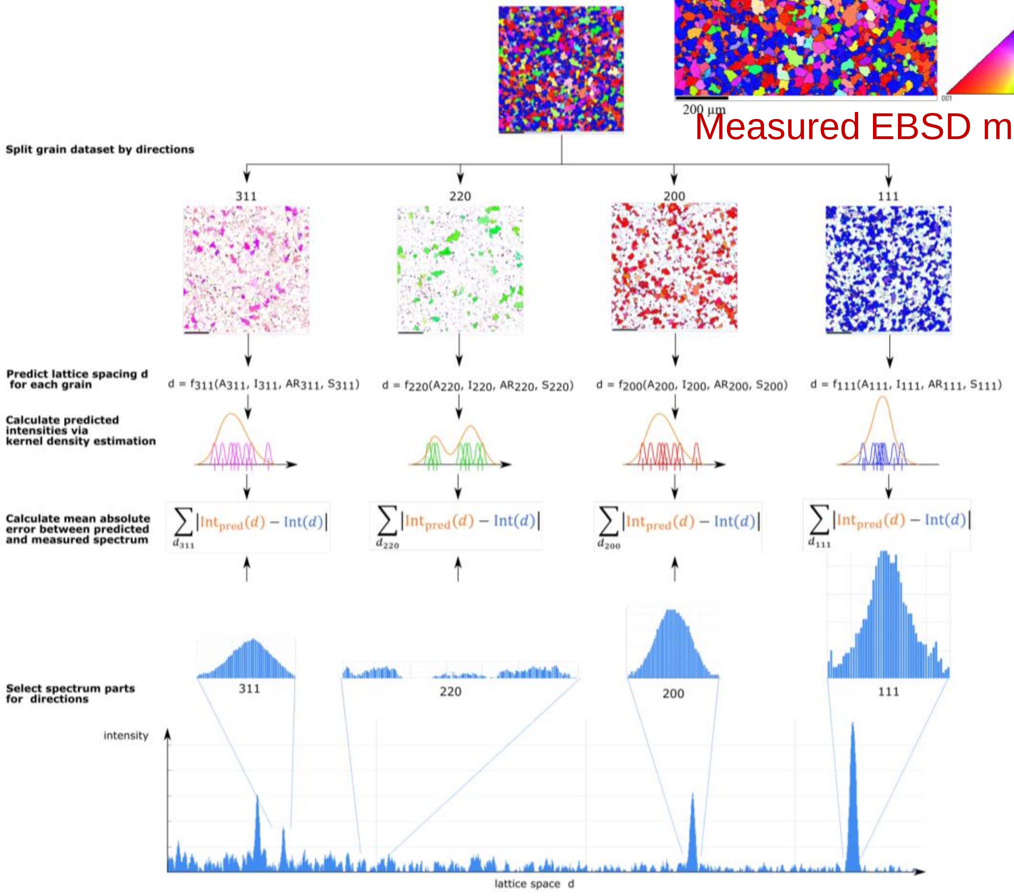

Overview of the GP learning process

A tree-like solution found by GP for the first model

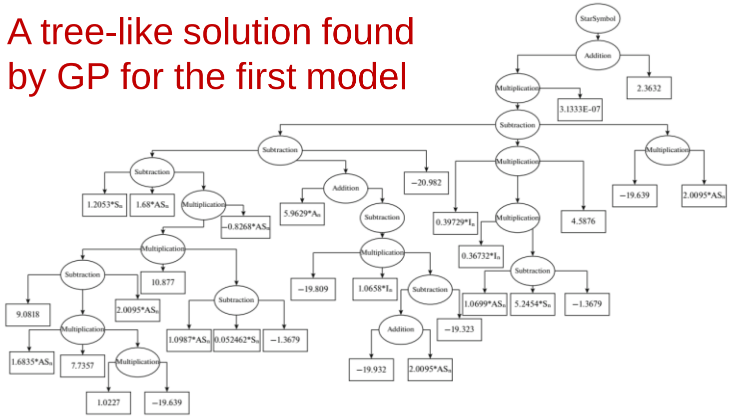

$$d^n_{hkl} = -0.5963 \cdot A_n - 0.6695 \cdot I_n^2 \cdot (1.0699 \cdot AR_n - 0.0525 \cdot S_n + 1.3679) - 21.1134 \cdot I_n \cdot (2.0095 \cdot AR_n + 39.2555) + 0.8268 \cdot AR_n \cdot (2823.2037 \cdot AR_n + 98.7866) \times (1.0987 \cdot AR_n - 0.0525 \cdot S_n + 1.3679) + 37.7815 \cdot AR_n + 1.2053 \cdot S_n + 23.3454$$

Solution found by GP algorithm

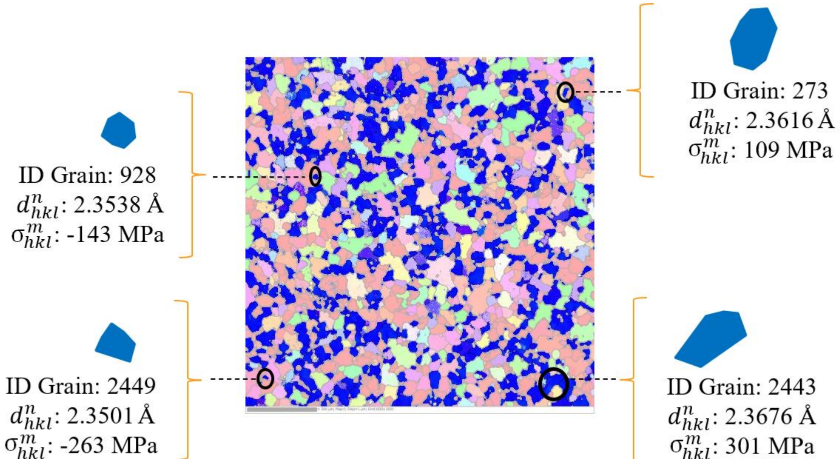

Lattice spacing and residual microstress values for some ⟨111⟩ grains calculated with the expression found by GP using HeuristicLab

[1] L. Millán, G. Bokuchava, R. Fernández, G. González-Doncel et al., **Journal of Materials Research and Technology**, 2023, V. 23, pp. 1543-1558.
[2] G. Kronberger, L. Millán, R. Fernández, G. Bokuchava, G. González-Doncel et al., **Applications in Engineering Science**, 2023, (accepted).

CRYSTALLOGRAPHIC TEXTURE OF MINERALS IN FOSSILS OF MOLLUSK SHELLS

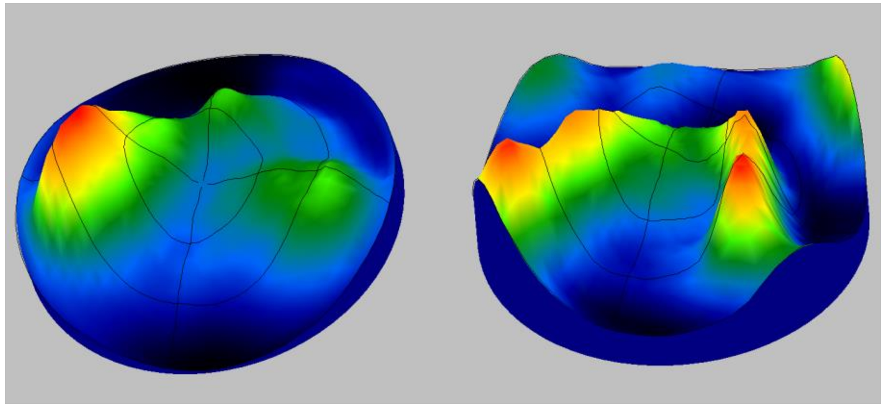

2.5D pole figures.

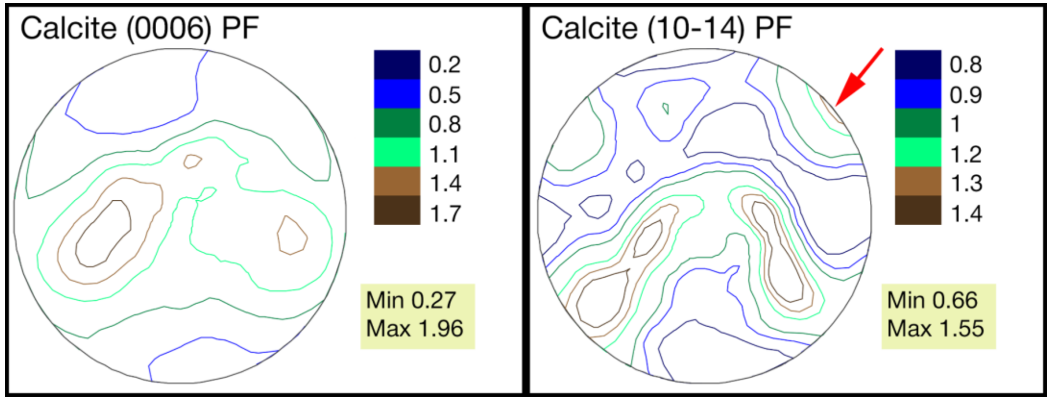

Pole figures of *Gryphaea dilatata* with features of recrystallization, quarry near the Sukhochevo village (6); red arrow – anomalous peak of maxima sharpness

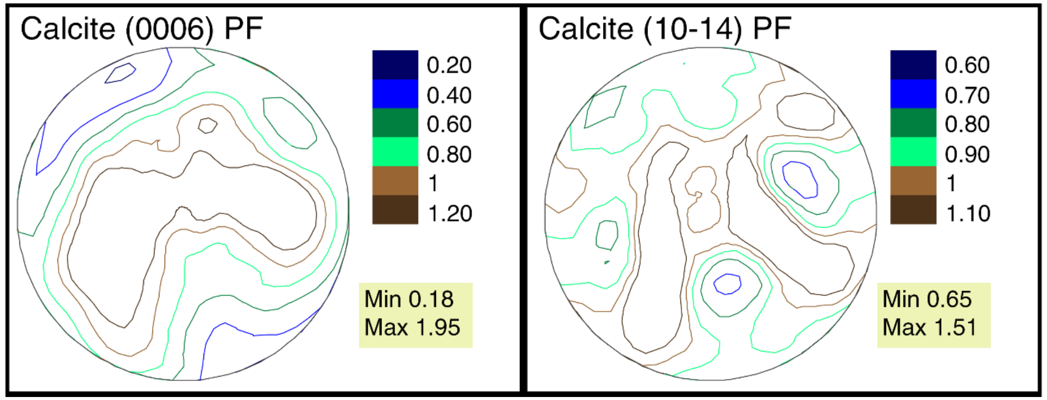

Pole figures of *Gryphaea dilatata* without the features of recrystallization, quarry near the Sukhochevo village (6)

A.Pakhnevich, Nikolayev, D.; Lychagina T., Biology, 2022, 11, 1300

A.V.Pakhnevich A.V., Nikolayev D.I., Lychagina T.N., Balasoiu M., Ibram O., Life, 2022, 12(5), 730.

Cultural Heritage Research by means of Neutron Tomography and Complementary Methods

Neutron tomography detector system

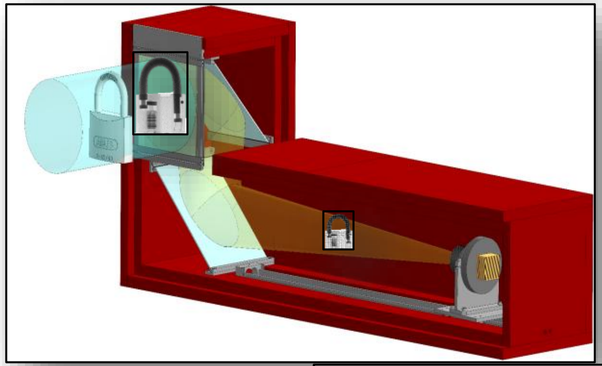

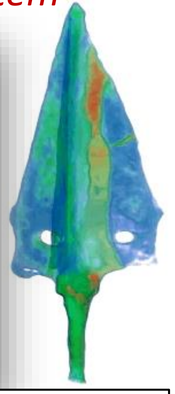

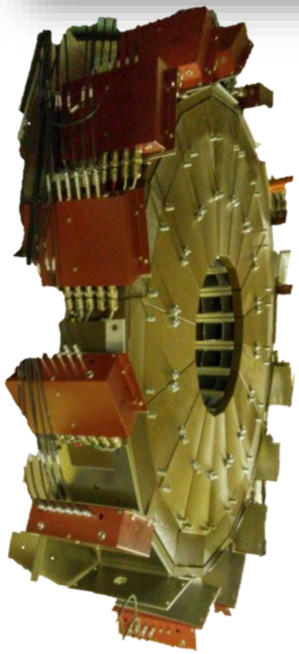

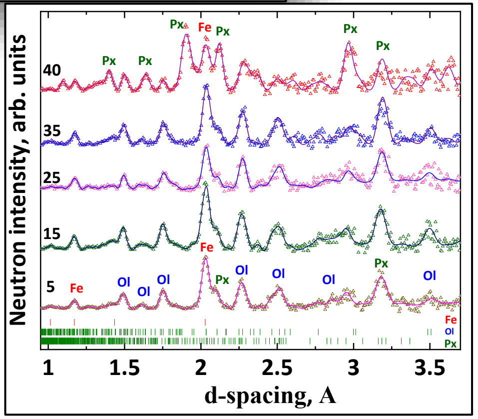

Neutron diffraction and Raman spectroscopy

Phase content and structural organization of antique coins

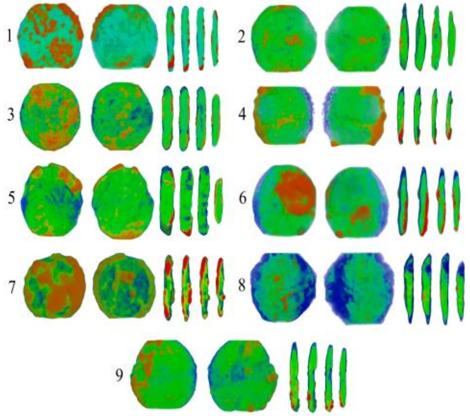

Internal construction and content of ancient jewelry objects

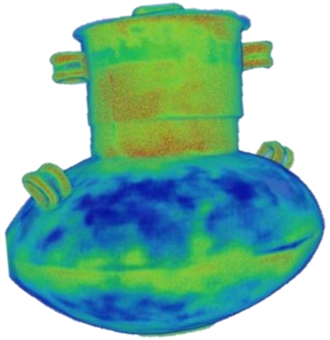

Phase content and structural organization of antique worship objects

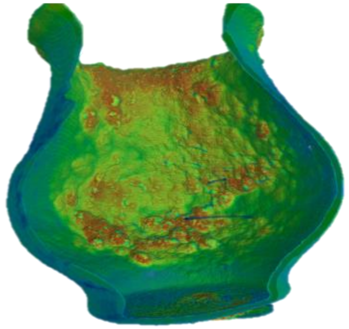

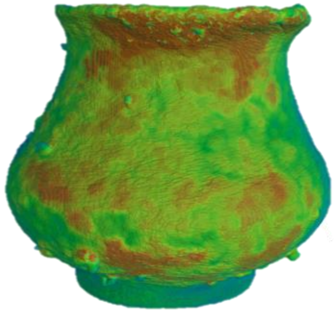

Cultural heritage objects of Dubna region

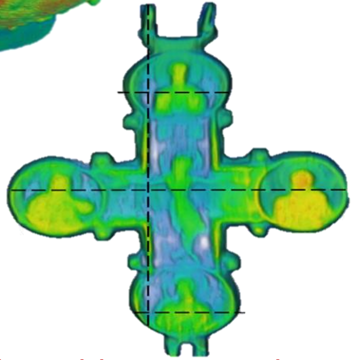

Ancient Russian cultural heritage objects

FURTHER DEVELOPMENT OF IBR-2 SPECTROMETER COMPLEX

Small-Angle Neutron Scattering/Neutron Radiography Spectrometer (SANSARA)

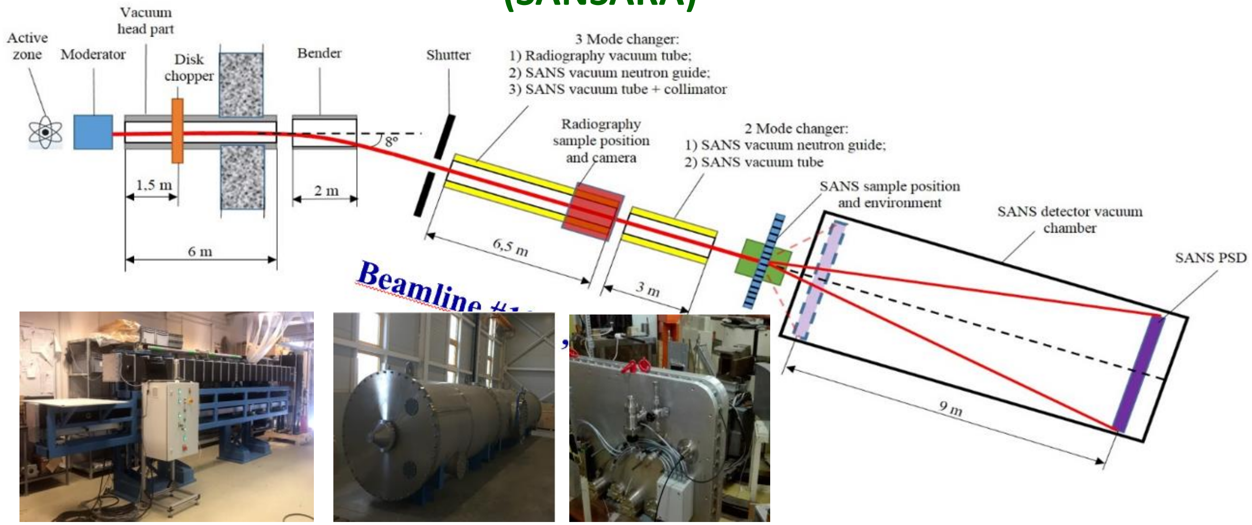

Inelastic neutron scattering spectrometer BJN

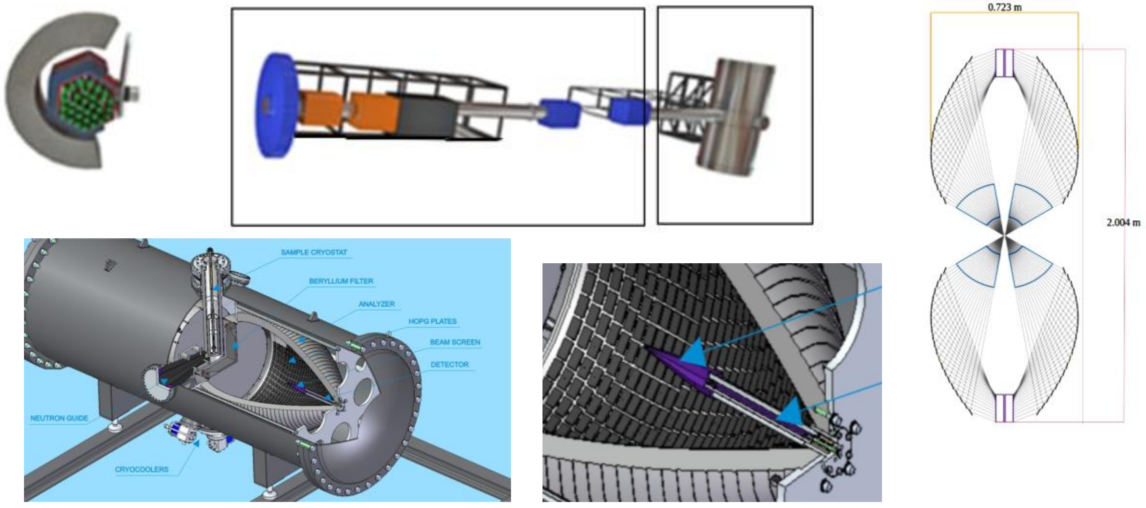

Construction of a wide-aperture backscattering detector (BSD-A) for the HRFD diffractometer

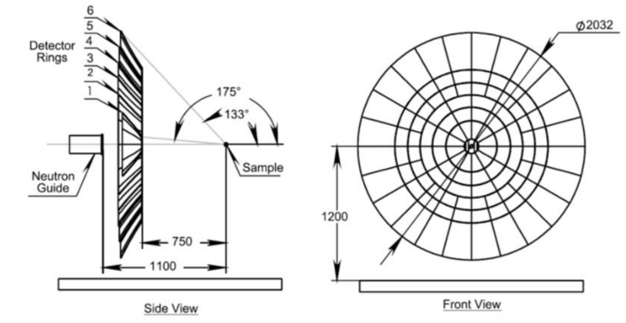

Summary

- В результате интенсивного развития методов рассеяния нейтронов на реакторе ИБР-2 была создана уникальная экспериментальная база для междисциплинарных исследований конденсированных сред.

- Ряд методических и научных результатов, полученных в разное время на установках ИБР-2, имел прорывной характер и оказал большое влияние на развитие методов рассеяния нейтронов в мире и формирование новых научных направлений на их основе.

- Экспериментальный опыт использования ИБР-2 сыграл большую роль в формировании концепции создаваемого в настоящее время European Spallation Source (ESS), развитии высокоинтенсивных методик малоуглового рассеяния, корреляционных методов дифрактометрии, дифрактометрии в режиме реального времени, методов исследований при воздействии высокого давления и др. нейтронных методов в других нейтронных центрах.

- В ходе проводимых исследований получена важная экспериментальная информация, оказавшая большое влияние на формирование и развития современных представлений в областях проводимых исследований.

- В настоящее время большинство установок ИБР-2 имеют параметры, соответствующие мировому уровню, отдельные установки являются передовыми в своих областях исследований.

- Реализация программы пользователей позволила организовать доступ заинтересованных исследователей из организаций как стран-участниц ОИЯИ, так и других стран к установкам реактора.

- Полученный опыт в создании установок и достигнутые результаты будут являться надежным фундаментом для развития экспериментальной базы и научной программы будущих нейтронных исследований в ЛНФ.

Thank You for Your Attention!